NUCLEAR RADIATION SHIELDING STUDIES
Report No. 1

A COMPARISON OF THEORY AND EXPERIMENT FOR SHIELDING BY A STRUCTURE AGAINST FALLOUT RADIATION

By
K. PREISS
and
A. B. CHILTON

A REPORT OF AN INVESTIGATION CONDUCTED
under the sponsorship of
THE OFFICE OF CIVIL DEFENSE
under
Contract OCD-OS-63-65

UNIVERSITY OF ILLINOIS
URBANA, ILLINOIS

June 1966

A COMPARISON OF THEORY AND EXPERIMENT FOR SHIELDING BY A STRUCTURE AGAINST FALLOUT RADIATION

by

K. Preiss and A. B. Chilton

Nuclear Radiation Shielding Studies

Report No. 1

June, 1966

A final report of an investigation carried out in the Department of Civil Engineering and the Nuclear Engineering Program, University of Illinois, for the Office of Civil Defense, Office of the Secretary of the Army, Washington, D. C., under Contract OCD-OS-63-66

Approved:

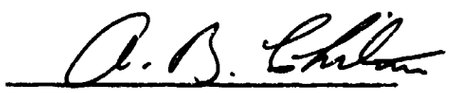

A. B. Chilton
Principal Investigator

SUMMARY

A comparison is made between experiment and theory for the calculation of shielding by a structure against fallout radiation.

Experimental results for exposure penetrating a roof slab, and for reduction factor, a r e found to agree with moments theory calculations, often to better than 10% when the geometry factor $L_a(\omega,X)$ was used.

A comparison between experiment and theory may be inaccurate due to anisotropy of the experimental source, to lack of source reflection in roof experiments, and due to error in estimating the thickness of the roof. The magnitudes of the errors due to these effects are investigated, and found to be small, but not necessarily negligible.

Detailed results of penetration in iron and concrete, due to plane isotropic sources of various energies are given, and a review of ground contribution to fallout radiation penetration through simple structures is appended.

CONTENTS

		Page
1	INTRODUCTION	1
2	THE LOGIC OF THE METHOD OF ANALYZING STRUCTURES FOR FALLOUT PROTECTION	2
3	ANALYSIS OF SOME POSSIBLE CAUSES OF EXPERIMENTAL ERROR	5
	3.1 Sources and Source Calibration	5
	3.2 Effect of Source Anisotropy in Free Field Measurements	7
	3.3 Effect of Lack of Source Reflection in Roof Experiments	9
	3.4 Errors in Estimating Roof Thickness	12
4	COMPARISON OF THEORY AND EXPERIMENT	13
	4.1 The Nuclear Defense Laboratory Blockhouse Experiment	13
	4.2 The Protective Structures Development Center Idealized Roof	19
5	CONCLUSIONS	21
REFERENCES		23
ACKNOWLEDGEMENT		24
FIGURES		25
APPENDIX A	CALCULATIONS OF EXPOSURE AND REDUCTION FACTOR DUE TO PLANE ISOTROPIC SOURCES IN IRON AND CONCRETE	32
APPENDIX B	A REVIEW OF GROUND CONTRIBUTION TO FALLOUT RADIATION PENETRATION THROUGH SIMPLE STRUCTURES	40
	B.1 Introduction	40
	B.2 Explanation of Situations Depicted	41
	B.3 Discussion and Conclusions	47
	B.4 Recommendations	50

1 INTRODUCTION

Standard methods of calculation of the protection afforded by a structure against fallout radiation depend upon the separation of the solution into a barrier and a geometry factor. These factors have been calculated in large part by moments theory, and have been presented as graphs[1,2].

The primary aim of the research project reported herein was to determine how valid the method of calculation is when applied to the case of fallout radiation on the roof of a structure. In order to do this, experimental work on the subject was reviewed and compared with theory. A number of reported experiments were examined and it was found that much of this work had been on structures such as houses and barracks which had very complicated geometrical configurations. Work reported on such structures gave values of radiation exposure valid only for the structure tested and accurate generalization of the results to other structures appeared to be extremely difficult. Since the aim of this project was to test the method of calculation of protection against fallout radiation, only those experiments which had been conducted on structures of reasonably simple geometry were used to compare with theory. The only such experiment reported at the time of writing was that at the Nuclear Defense Laboratory[3]. Preliminary results from work at the Protective Structures Development Center[4] were also available.

To provide a comparison between theory and experiment, it was necessary to compute the exposures due to a plane isotropic source penetrating steel slabs, since steel slabs were used in the NDL experiment and calculations for steel using moments theory were not available. At the same time, calculations were done for concrete and for air, for a plane isotropic source, at several energies.

Three factors which may cause error in comparison of theory and experiment were considered. These are the effect of source anisotropy in free field measurements, the effect of lack of source reflection in roof experiments, and the effect of error in estimating the thickness of the slab used in the experiment. The order of magnitute of errors due to the above

three factors were estimated and they were found generally to be small but not necessarily negligible, as reported in Section 3.

The experimental measurements available[3,4] were not corrected for these effects in this report. The experimental results were compared with the theoretical exposures and reduction factors calculated here (see Appendix A); agreement was often better than 10%.

In the appendices, two subjects of related interest which arose during this investigation are reported. These are the detailed results of exposure distributions and reduction factor calculations in iron and concrete due to plane isotropic sources of various energies, calculated by moments theory; and a review of ground contribution to fallout radiation penetration through simple structures.

2 THE LOGIC OF THE METHOD OF ANALYZING STRUCTURES FOR FALLOUT PROTECTION

Before proceeding with a comparison of theory and experiment, it is helpful to know where the theory fits into engineering technology and how experiment relates to the theory. The relation of theory and experiment are discussed in this Section, together with some general considerations.

In engineering design, the properties of a structure or other item are specified, and the components are then selected and proportioned so as to give the required results; in analysis, a structure is completely specified and then some property, such as its behavior under an unusual condition, is calculated.

If a calculation method is available which permits direct computation of the size and specifications of the structure to satisfy the design criteria, then the structure may be directly designed. Many structures cannot be directly designed. The procedure then is to select a design, analyze it, amend the design to satisfy some given criteria, analyze again, and so on. We then have a feed-back interative process where analysis is one part of the design procedure.

The hypothetically most accurate and direct approach to the problem of analyzing a structure for its ability to shield people from fallout radiation would be to subject it to actual fallout and measure the

exposure received. This is not practical, nor is it practical to subject every structure to simulated fallout radiation.

For this reason, structures are divided into classes, categorized by some general properties such as size, construction material, etc. This implies that we know which properties are significant for this problem, and which are not, so that the process of generalization has small effect on the accuracy of the analysis.

It is not practical to do experiments which cover all relevant regions of all relevant variables even within one class of structure. Recourse is then made to theory, which is a generalization of the practical problem in a way that can be applied with reasonable effort and accuracy to any structure in the class to which it pertains.

Before the theory of radiation protection can justifiably be used, it must be established for which situations it is applicable and how accurate it is. This is done by comparing theory with experiment, and the experiment must be as careful and as accurate as possible so that it gives some evidence as to the validity of the theory. Once that is established, the theory may be used with an established degree of confidence, for any particular problem.

Since the biological effects of radiation dose are relatively insensitive to small changes of dose, great accuracy in the knowledge of the shielding capability of any one structure is superfluous. If, therefore, an experiment were performed on a structure simply to obtain the protection factor of that structure, it need not be extremely accurate. But if it is performed to check a theory, it must be well understood and carefully carried out, so as to give limits of confidence to the theory. By this means a small number of careful experiments, linked to a theory, can replace much random empiricism.

In order to draw conclusions about the method of calculation for analyzing structures against fallout radiation, it is convenient to consider both the experimental and practical situations, and the theoretical model, in five parts (see Table 1):

(1) The spatial distribution of the source;

(2) The nuclear properties of the source;

(3) The spatial distribution of the structure;

(4) The nuclear properties of the structure;

(5) The definition of the dependent variable, exposure.

These five aspects are discussed below.

(1) It is assumed that real fallout will be uniformly distributed in plan. The validity of this assumption is not discussed in this report. The source is treated as a uniform plane in theory, and this can be accurately simulated by experiment.

(2) The interactions of gamma radiation with matter are well understood over the relevant energy range. Conclusions drawn about the theory on the basis of experiments with sources other than fallout may therefore be taken as valid for application to real situations. There is some difficulty in knowing just what to consider to be the source properties in an experiment, on account of the fact that experimental sources are often large relative to the mean-free-path length of radiation within them, and because in calculations using moment theory to find the penetration through a roof slab the exposure originating from fallout on the ground (skyshine) is not separated from the exposure originating from fallout on the roof. This is discussed in Section 3.

(3) The theory assumes the roof of the structure to be an infinite homogeneous slab whereas real structures consist of columns, walls, beams, and finite slabs. This is the major point of difference between theory and reality, and experiments should be, and are, designed to check the validity of the theory in different geometries of structures.

The material geometries of the experiment correspond to those of real structures. In order to use experimental evidence to draw conclusions about the relevance of theory to reality, differences in source spectra between experiment and theory must be accounted for.

(4) Nuclear properties of structural materials with respect to gamma radiation are known. The effect of the small inaccuracies in available

nuclear data is much less than the effect due to the relatively large dimensional tolerances allowed in the sizes of structural members.

(5) The detectors used in experiment measure exposure. This is the dependent variable in the theory. It is worth pointing out that the absolute calibration error of even the best detector is of the order of 2% or more, and some detectors used have inaccuracies an order of magnitude greater.

Table 1 shows in summary form the areas of similarity and dissimilarity as discussed above.

TABLE 1

Summary of relation of theory and experiment to assumed real situation.
0 represents similarity to assumed real situation
X represents difference compared with assumed real situation

Property	Theory	Experiment
(1) Source, Spatial	0	0
(2) Source, Nuclear	0	X
(3) Structure, Spatial	X	0
(4) Structure, Nuclear	0	0
(5) Detector response	0	0

3 ANALYSIS OF SOME POSSIBLE CAUSES OF EXPERIMENTAL ERROR

3.1 Sources and Source Calibration

The reduction factor of a structure is expressed as the ratio of the exposure observed at a given point in a structure to the exposure which would be observed three feet above a smooth, infinite, unobstructed, uniformly contaminated plane. Experimentally these exposures are derived from separate measurements. Each exposure is normalized to an arbitrary

source strength, usually 1 curie/ft^2, and the ratio then taken. The protection factor is defined as the reciprocal of the reduction factor.

If the same source were used for the structure and the free field experiment, and if it were isotropic there would be no need to normalize the dose to a source strength, because the exposure observed in the structure divided by the free field exposure would be the protection factor. If an anisotropic source were used in either experiment, normalization of the observed exposure to a calibrated source strength would require that the source anisotropy be allowed for.

In practice, the sizes of the sources and capsules used are not small compared with the mean-free-path length of radiation in them, nor are they spherically symmetrical. This leads to two effects:

(a) Degradation of the source spectrum;

(b) Anisotropy of the emitted exposure with respect to the source orientation.

When the source is calibrated in air, the low energy components of the spectrum are detected. When the source is placed on a barrier, the low energy components are more rapidly attenuated than the higher energy components. If the results are compared with a theory derived for the source energy, the theory will overestimate the transmitted exposure.

Berger and Doggett[5] compared their calculations with an experiment of Kirn, Kennedy, and Wyckoff[6] and concluded that neglect of the energy degradation from a 1 cm thick Co-60 source gave rise to an overcalculation in exposure of 18 ±5% for barriers approximately 120 psf thick.

The error introduced in an experiment by neglecting the degraded source spectrum can be estimated if the source spectrum is known, by using the penetration calculations for various incident energies given in this report in Appendix A. Unfortunately the source spectra were not determined for sources used in the experiments. This effect may in fact turn out to be small in some experiments but no firm evidence is available to allow this assumption.*

*A program to calculate by Monte Carlo methods the spectrum of gamma radiation emitted from a source is at the present time being written, and when available it should help to solve this problem.

The experimental value of exposure in air three feet above the source plane is obtained by measuring the exposure, either when the source is pumped through a tube on the ground, or by placing a detector in many locations when a source is placed in one location and the results summed to simulate a plane field. An estimate of the effect of source anisotropy in the latter procedure is made in Section 3.2.

3.2 Effect of Source Anisotropy in Free Field Measurements

The free field measurements made at the Nuclear Defense Laboratory[7] had been carried out by placing detectors in a number of positions relative to a single source on a field and summing the observed exposures to simulate an infinite plane source. Since the source was probably not isotropic, the observed exposure, when normalized to the calibrated source strength, may have been in error. An estimate of the error due to this effect was made as follows.

Since the anisotropy of the source radiation was not known for the sources used at the Nuclear Defense Laboratory, an estimate of the order of magnitude of the effect was made for a hypothetical case, using the reported exposure distribution around a Co-60 source, given by Burson and Summers[8] and shown in Fig. 1.

The reduction factor due to area A of Co-60 in a field is given by

$$\frac{D}{D_o} = P(d)\, A/4\pi d^2 \qquad 3.2.1$$

where A and d are shown in Fig. 2 and P(d) for Co-60 is given in Fig. B-19 of the monograph by Spencer[1]. Referring to Fig. 2, this can be written for a plane isotropic source

$$\frac{D}{D_o} = \int_o^\infty P(d)\, 2\pi r\, dr/4\pi d^2 \qquad 3.2.2$$

The exposure emitted by the Co-60 source shown in Fig. 1 can be written, with some approximation as

$$F(\theta) \equiv \frac{D_\theta}{D_c} = \begin{cases} (1 - 0.0033\,\theta), & -60^\circ < \theta \leq 60^\circ \quad \text{3.2.3a} \\ 0.5, & 60^\circ < \theta \leq 90^\circ \quad \text{3.2.3b} \end{cases}$$

Including this anisotropy effect in eq. 3.2.2 gives an approximate relation

$$\frac{D}{D_o} \approx \int_o^\infty F(\theta)\, P(d)\, r\, dr/2d^2 \qquad \text{3.2.4}$$

where D is now the exposure at the detector due to a uniform infinite contamination corresponding to a calibrated source intensity D_c ; the source energy is here assumed to be 1.25 MeV with no degradation.

Changing variables, the relative exposure due to an infinite plane source is

$$\frac{D}{D_o} = \frac{1}{2} \int_1^0 F(\theta)\, P(d)\, \frac{d(\sin\theta)}{\sin\theta} \qquad \text{3.2.5}$$

To find the effect of source anisotropy, the ratio

$$\frac{\frac{1}{2} \int_0^1 F(\theta)\, P(d)\, \frac{d(\sin\theta)}{\sin\theta}}{\frac{1}{2} \int_0^1 P(d)\, \frac{d(\sin\theta)}{\sin\theta}}$$

was calculated and found to be 0.96 .

This calculation shows that if free field measurements were done by the method described by Rexroad and Schmoke[7] using a source similar to that described by Burson and Summers[8], source anisotropy would decrease

the measured relative exposure by approximately 4% . If the source were such that the exposure on the axis were greater than that observed normal to the axis, source anisotropy would increase the relative exposure.

3.3 Effect of Lack of Source Reflection in Roof Experiments

The barrier and geometry factors in present methods of calculation of fallout protection are calculated usually by the method of moments. These assume, among other things, an infinite extent of material on that side of the source which is away from the detector.

In reality, fallout would be in a thin layer on and around a structure with air above it. If the fallout field were infinite in extent, or greater than three mean-free-path lengths (about 1500 feet) in radius, and if the building height were small compared with a mean-free-path length in air, then the contribution of radiation scattered from the air above would equal the theoretical contribution due to the radiation scattered back by the hypothetical infinite medium.

If the source in a roof experiment were covered with an infinite thickness of the same material as the roof, the experimental configuration would be identical with the theoretical source configuration in the moments calculations, and this would include the equivalent of "skyshine." Since this was not always the case in past experiments, an estimate must be made of how much the theory may have differed from the experimental results on account of the experimental source characteristics.

Berger and Doggett[5] calculated build-up factors for finite and semi-infinite barriers for plane normal sources. The difference between the results for the two barriers, for a 1 MeV source on iron, at one mean-free-path, was 1% . For an isotropic source, the difference may be expected to be larger.

An approximate calculation can be made as follows: From the results presented in Appendix A the exposure penetrating into iron from a 1.25 MeV plane isotropic source is known. We wish to subtract the exposure due to the radiation which moves initially away from the detector and then crosses the source plane to be detected.

A COMPARISON OF THEORY AND EXPERIMENT FOR SHIELDING BY A STRUCTURE AGAINST FALLOUT RADIATION

by

K. Preiss and A. B. Chilton

Nuclear Radiation Shielding Studies

Report No. 1

June, 1966

A final report of an investigation carried out in the Department of Civil Engineering and the Nuclear Engineering Program, University of Illinois, for the Office of Civil Defense, Office of the Secretary of the Army, Washington, D. C., under Contract OCD-OS-63-66

Approved:

A. B. Chilton
Principal Investigator

SUMMARY

A comparison is made between experiment and theory for the calculation of shielding by a structure against fallout radiation.

Experimental results for exposure penetrating a roof slab, and for reduction factor, a r e found to agree with moments theory calculations, often to better than 10% when the geometry factor $L_a(\omega,X)$ was used.

A comparison between experiment and theory may be inaccurate due to anisotropy of the experimental source, to lack of source reflection in roof experiments, and due to error in estimating the thickness of the roof. The magnitudes of the errors due to these effects are investigated, and found to be small, but not necessarily negligible.

Detailed results of penetration in iron and concrete, due to plane isotropic sources of various energies are given, and a review of ground contribution to fallout radiation penetration through simple structures is appended.

Berger and Raso[10] give the following values for the number albedo A from a 1.25 MeV isotropic source: on iron 0.295 ; on concrete 0.383.

Berger and Raso[9] calculated the reflected energy spectrum for a 1 MeV isotropic source on iron. This is shown in Fig. 3. On the basis of this result, it will be assumed that all the reflected photons due to a Co-60 source on iron or concrete have energy 0.25 MeV .

The current due to scattered radiation which crosses the source plane will be A times the source current and is assumed to be at 0.25 MeV . Assuming, without justification, that this is isotropic at the source plane, the penetration of the scattered radiation can be found from the moments calculation at 0.25 MeV . The exposure at depth Z psf in the barrier, due to reflection above the source, will be

$$\frac{A \cdot D(Z,\ 0.25\ \text{MeV})}{D(Z,\ 1.25\ \text{MeV})} \quad .$$

This calculation will be approximate, because the reflected photon distribution will be more peaked than isotropic and because the energies of the reflected photons are not at a single energy, but an estimate of the order of magnitude of the effect is obtained from this calculation. The calculated ratios of exposure reflected by source cover to exposure in an infinite medium, are shown in Table 2.

The above calculation gives approximately the same result as calculations using the functions given by Spencer[1]. In his notation:

S(d) is the ratio of exposure due to radiation from the upper hemisphere ("skyshine") to the reference exposure 3 feet in air above the source plane;

S'(X) is the ratio of exposure at X psf to the exposure at 0 psf, due to a plane source in an infinite medium, emitting radiation isotropically into the half-space in which the detector is buried;

L(X) is the ratio of exposure due to a plane infinite isotropic source, at X psf in an infinite medium, to the reference exposure 3 feet in air above the source plane.

A comparison between the two methods of calculation is obtained by comparing the value of $\frac{A \cdot D(Z,\ 0.25\ MeV)}{D(Z,\ 1.25\ MeV)}$ in the previous calculation with $\frac{S(d)\ S'(X)}{L(X)}$ in this calculation, when $d = 0$. Note that both calculations refer to infinite source planes; solid angle fraction ω is then one and $S_a(X,\omega) = 1$.

The latter approach was used by Raso and Woolf[17] when comparing their Monte Carlo calculations of roof contributions with the moments calculations of Spencer[1]. When the quantity $S(d)\ S'(X)\ S_a(\omega,d)$ was subtracted from the value of $L(X)\ L_a(X,\omega)$, good agreement was found with the Monte Carlo results.

TABLE 2

Ratio of exposure reflected by source cover to total exposure for iron and concrete. Results from approximate calculation, using albedo and penetration curves; and using curves of NBS 42[1].

Material	Z PSF				Calculating Procedure
	25	50	100	150	
Iron	0.025	0.011	0.003	0.0005	$\frac{A \cdot D(Z,\ 0.25\ MeV)}{D(Z,\ 1.25\ MeV)}$
Concrete	0.062	0.037	0.013	0.004	
Concrete	0.077	0.060	0.031	—	$\frac{S(d)\ S'(X)}{L(X)}$; d=0

The results of the two methods of calculation are given for concrete in Table 2 and show reasonable agreement at low barrier thicknesses, when the correction is more significant; at greater thicknesses agreement is not as good, but the correction is then not important.

The calculations show that lack of source reflection may account for about 3% of the exposure in iron and 6% in concrete at 25 psf, about 1% in iron and 4% in concrete at 50 psf, and less at greater distances. This difference between theory and experiment may be avoided simply by having a reflector over the source.

3.4 Errors in Estimating Roof Thickness

During the course of this investigation, a question arose as to the error provoked when relating theoretical to experimental exposures, by assuming that a slab has exactly the nominal thickness when in fact it may not have. An extimate of this cause of error is made as follows.

Consider a roof slab, upon which is placed a uniformly distributed plane isotropic source. The radiation exposure within the slab can be approximately given by $D = D_o e^{-\mu t}$ when t is the slab thickness and μ is the effective broad beam attenuation coefficient for the slab. The relation between errors in D and t is given by $\frac{\delta D}{D} = \mu\, \delta t$. 3.4.1

The effective broad beam attenuation coefficient for a plane isotropic Co-60 source on steel is found from Fig. A2 of Appendix A to be 0.027 psf^{-1} , or 1.1 $in.^{-1}$ Assuming this is known with zero error $\frac{\delta D}{D} = -1.1\, \delta t$ where t is in inches. 3.4.2

The difference between real and nominal thicknesses is demonstrated by observations made during an unpublished experiment at the University of Illinois. Sheets of glass, graphite, aluminum, and lucite, each 4.5 sq. ft. in area and nominally 1" thick, were measured on a 6" sq. grid. The mean dimensions found are shown in Table 3.

TABLE 3

Measured thickness of nominal 1" material. The mean of 18 micrometer readings is given

Material	Thickness (inches)
Aluminum	0.980
Glass	1.005
Lucite	0.967
Graphite	1.002

The American and Iron Steel Institute[12] gives the rolling tolerances for structural plates to be minus 0% plus 7% . If we assume that steel

used in an experiment is 3% thicker than the assumed nominal value, then $\delta t = 0.03 \times t$ and the observed exposure will be decreased by

$$\frac{\delta D}{D} = 1.1 \times .03 \times t$$
$$= 0.03 \times t \qquad 3.4.3$$

The observed exposure will then decrease by about 3% for each inch thickness of steel.

4 COMPARISON OF THEORY AND EXPERIMENT

4.1 The Nuclear Defense Laboratory Blockhouse Experiment[3]

In this experiment sources of Co-60 and Cs-137 were placed on the roof of a blockhouse so as to simulate a plane source; detectors were placed within the blockhouse and exposures were measured. In a separate experiment, the same sources were placed [illegible]en field and the exposure three feet above the effectively infinite [illegible] source measured. Dividing the former exposure by the latter gave the reduction factor.

The blockhouse had internal dimensions 12 ft by 12 ft by 8 ft high. The walls were of concrete, 4 inches thick. The roof, which was supported by the walls and by a joist at the blockhouse center line, consisted of 1/2 inch plywood, and various thicknesses of steel or concrete above this. The source rested on a 1/2 inch thickness of lucite on the roof.

The detectors were Victoreen Model 208 10mr dosimeters. These were calibrated to ±2% against a Victoreen Model 130 r-meter which itself had been calibrated to ±2% at the National Bureau of Standards. Twenty-four detectors were placed within the blockhouse at various positions.

The sources used were 0.34 curies of Co-60 and 1.35 curies of Cs-137. The cobalt was metal in a stainless steel capsule; the cesium was CsCl also in a stainless steel capsule. The sources were calibrated by holding them a known distance from NBS-calibrated ion chambers. The calibration of the ion chambers was accurate to ±2% , and it is expected that the calibration of the source relative to the ion chambers was accurate to about 2% , so the source calibration was probably accurate to

$$\sqrt{(0.02)^2 + (0.02)^2} \approx 3\% \ .$$

Each source was placed on the roof in a number of locations and the exposure rates thus observed were summed so as to be equivalent to a uniform source distribution on the roof.

The experimental exposures at various heights on the blockhouse center lines were compared with theoretical values by the NDL workers, in the following way:

(a) The exposures observed with a steel roof were multiplied by a factor of 1.11 to make them equivalent to those which would be observed with a concrete roof. The factor 1.11 was used as the average ratio of ordinates of the curves of exposure vs effective mass in concrete and iron for a 1 Mev plane normal source (Fig. 22.1 of reference 1).

(b) The reduction factor was calculated by dividing this exposure rate by the exposure rate D_o, observed three feet above an infinite contaminated field. The values of D_o were observed in previous work at the same site.[7]

(c) The theoretical reduction factor was taken from Fig. 28.19 of NBS 42[1], which gives values of $L(X)\ L_a(X,\omega)$ calculated for water and a 1.12 hr fission source.

Comparison of those experimental results with theory was repeated in this investigation, making use of the newly computed penetrations in steel (see Appendix A) and using a procedure as follows:

(a) Roof thicknesses were expressed as actual pounds per square foot Z, not as equivalent mass thickness X (see Appendix A).

(b) The experimental exposure rates for steel roofs given in Tables 3.1 and 3.2 of the NDL report in roentgen/hr per curie/ft^2 were divided by 1.11, so as to eliminate the "correction" previously made. The sources had been calibrated using specific gamma ray constants of 14.3 roentgen/hr at one foot from a curie of Co-60 and 4.2 roentgen/hr at one foot from a curie of Cs-137. The values corresponding to 86.9 roentgen per erg/gm are 14.0 roentgen/hr at one foot from a curie of Co-60 and 3.4 roentgen/hr at one foot from Cs-137. The values of exposure rate per curie, used in the theory and in the reduction of experimental data, were made equal.

(c) The exposures obtained from the moments calculation for 1.25 MeV were multiplied by 5284 to convert from MeV/gm per photon/cm^2 to roentgen/hr per curie/ft^2. This constant is obtained as follows:

1 MeV = 1.602×10^{-6} erg

1 roentgen = 86.9 erg/gm

1 curie of cobalt = 7.4×10^{10} photons/sec

1 ft^2 = 929.03 cm^2

Thus, 1 MeV/gm sec per photon/cm^2 sec

$$= \frac{1.602 \times 10^{-6}}{86.9} \times \frac{7.4 \times 10^{10}}{929.03} \times 3600$$

= 5284 roentgen/hr per curie/ft^2

Since cesium-137 emits 0.84 photons per disintegration whereas cobalt-60 emits two photons per disintegration, the conversion factor for cesium-137 will be 2219 roentgen/hr per curie/ft^2.

(d) The geometry factors $L_a(\omega,X)$ and $L_c(\omega,X)$ were obtained from Figs. B27, B28, B29, and B30 of NBS 42[1], which are for Co-60 and Cs-137 in concrete. Geometry factors have not been calculated for steel, because it is expected that these factors will be much less dependent on the difference between mass attenuation coefficients for steel and concrete than the barrier factor.

(e) The theoretical exposure rates were computed from $D(Z)L_a(\omega,X)$ and $D(Z)L_c(\omega,X)$, where $D(Z)$ was obtained as shown in (c) above. These are compared with the NDL observations in Table 4.

(f) The reduction factor was calculated by dividing the exposure rate obtained in (e) above by the calculated exposure in the air three feet above the ground as shown in Appendix A. These calculations are compared with the NDL observations in Table 5.

Tables 4 and 5 and Figures 4 through 7 show the calculated and observed exposure rates and reduction factors. The curves are not plotted beyond 45 psf because the observations at 50 psf were for a concrete roof, whereas the other observations and calculations are for steel.

There are several possible causes of error in comparing theory to experiment; since these were not all evaulated in the report[3] an order of magnitude estimate of these errors is made here.

TABLE 4

Ratio of Theoretical Exposure Rate

(mr/hr per curie/ft^2) to Observed Exposure Rate

Source	Detector Location	ω	Barrier Thickness PSF				Theoretical Geometry Factor Used
			18.0+	33.7+	44.9+	50.3*	
Co-60	C 6	0.73	1.08	1.08	1.09	0.98	$L_a(\omega, X)$
	C 3	0.41	0.97	1.03	1.08	0.97	
	C 0	0.24	0.74	0.83	0.92	0.83	
	C-1	0.20	0.79	0.86	0.85	0.78	
Co-60	C 6	0.73	1.17	1.26	1.29	1.22	$L_c(\omega, X)$
	C 3	0.41	0.95	1.07	1.18	1.17	
	C 0	0.24	0.72	0.83	0.98	0.94	
	C-1	0.20	0.75	0.84	0.91	0.90	
Cs-137	C 6	0.73	1.06	1.12	1.26	1.13	$L_a(\omega, X)$
	C 3	0.41	1.06	1.02	1.06	1.03	
	C 0	0.24	0.97	0.91	0.92	0.90	
	C-1	0.20	0.98	0.87	0.91	0.94	
Cs-137	C 6	0.73	1.26	1.37	1.55	1.45	$L_c(\omega, X)$
	C 3	0.41	0.96	1.25	1.35	1.43	
	C 0	0.25	0.81	1.03	1.11	1.22	
	C-1	0.20	0.78	0.97	1.06	1.18	

+ Steel was used in the experiment for these thicknesses.

* Concrete was used in the experiment for this thickness only.

TABLE 5

Ratio of Theoretical Reduction Factor
to Observed Reduction Factor

Source	Detector Location	ω	Barrier Thickness PSF				Theoretical Geometry Factor Used
			18.0+	33.7+	44.9+	50.3*	
Co-60	C 6	0.73	1.00	1.00	1.00	1.02	$L_a(\omega, X)$
	C 3	0.41	0.82	0.95	1.00	1.03	
	C 0	0.24	0.69	0.77	0.84	0.85	
	C-1	0.20	0.71	0.74	0.81	0.78	
Co-60	C 6	0.73	1.09	1.17	1.20	1.26	$L_c(\omega, X)$
	C 3	0.41	0.80	0.98	1.09	1.22	
	C 0	0.24	0.67	0.77	0.91	0.96	
	C-1	0.20	0.71	0.74	0.85	0.91	
Cs-137	C 6	0.73	0.94	1.00	1.13	1.10	$L_a(\omega, X)$
	C 3	0.41	0.94	0.91	0.97	0.99	
	C 0	0.24	0.87	0.81	0.82	0.87	
	C-1	0.20	0.86	0.79	0.84	0.94	
Cs-137	C 6	0.73	1.12	1.22	1.39	1.42	$L_c(\omega, X)$
	C 3	0.41	0.86	1.11	1.20	1.42	
	C 0	0.24	0.71	0.91	1.00	1.17	
	C-1	0.20	0.70	0.86	0.95	1.17	

+ Steel was used in the experiment for these thicknesses.

* Concrete was used in the experiment for this thickness only.

(a) The error in the calculated values was of the order of 2% due to difficulties in reading accurately the values of $L_a(\omega,X)$ and $L_c(\omega,X)$ from the graphs in NBS 42[1];

(b) Uncertainty in absolute calibration of the source strength is expected to have been approximately 3% (see text);

(c) Because of anisotropy of the source in free field measurements[7], D_o for Co-60, when expressed as exposure rate per curie/ft^2, may possibly have been in error by approximately 4% (see Section 3.2);

(d) If the Co-60 source were entirely unreflected then the theoretical exposure rate would have been higher than the experimental exposure rate by approximately 2% at 25 psf and 1% at 50 psf in steel (see Section 3.3). Since in fact the finite size of the source would have caused some radiation to be reflected back into the roof this effect may have been small, for the steel roofs tested. For concrete, the effect would have been larger, but still small;

(e) The nominal thicknesses of the steel roofs appear to have been used for the calculations in the NDL report. It is possible that the thicknesses were in fact greater than nominal. If they were 3% thicker the exposures would have been overcalculated by approximately 1% at 18 psf, 2% at 34 psf and 3% at 45 psf for the Co-60 source (see Section 3.4);

(f) Because of degradation of the source spectrum, the measured values of exposure rate per curie/ft^2 through the barrier would have been lower than the theoretical values. The magnitude of this effect is, for the present, unknown (see footnote to page 6).

The effect listed in (c) above would have reduced or increased the free field exposure rate, depending upon the geometry of the encapsulated source, whereas those listed in (d), (e), and (f) above would have decreased the exposure rate observed in the blockhouse. This discussion of possible errors is based on general considerations and no judgement can be given here as to whether these causes of difference between theory and experiment were actually present.

Agreement between calculated and observed reduction factors appears to be better for larger solid angles and greater barrier thickness, and better agreement is found between theory and experiment when the geometry factor $L_a(\omega,X)$ is used than when the factor $L_c(\omega,X)$ is used.

The geometry factor $L_a(\omega,X)$ is calculated for an infinite plane source in an infinite medium and a limited solid angle of detector response; the factor $L_c(\omega,X)$ is calculated for a circular plane source in an infinite medium and a detector response over 4π steradiams. Since in fact the barrier has a finite thickness, and the detector is some distance from the barrier with only air in its close vicinity, the factor $L_a(\omega,X)$ may indeed be expected to give more accurate results.

Of the 16 values of reduction factor calculated for Co-60 (using $L_a(\omega,X)$):

7 fall within ± 10% of experiment;

11 fall within ± 20% of experiment;

15 fall within ± 30% of experiment.

For Cs-137 (using $L_a(\omega,X)$):

8 fall within ± 10% of experiment;

15 fall within ± 20% of experiment.

4.2 The Protective Structures Development Center Idealized Roof[2]*

In this experiment, a circulating source was placed on the ground with concrete slabs above. Detectors were placed at various heights above the slabs.

The reduction factors were calculated by dividing the observed exposure rates by the exposure rates previously measured three feet above an infinite plane of contamination. These experimental reduction factors were compared with the theoretical values of $L(X)L_a(X,\omega)$ and $L(X)L_c(X,\omega)$ and this comparison is repeated here by taking the values given in that report.[4]

---

*At the time of this writing, preliminary results only are available.

The $L(X)L_a(X,\omega)$ curves were closer to the observed results than the $L(X)L_c(X,\omega)$ curves, at all values of X. The differences are listed in Table 6.

TABLE 6

Comparison of Theory and Experiment for the PSDC Idealized Roof.
Ratio of Calculated Reduction Factor to Observed Reduction Factor

Barrier PSF	ω	Theoretical Value	
		$L(X)L_a(\omega,X)$	$L(X)L_c(\omega,X)$
0	0.02	1.00	0.95
	0.10	1.00	0.94
	0.60	1.00	0.94
48	0.02	1.12	1.19
	0.10	1.15	1.25
	0.60	1.17	1.43
96	0.02	1.07	1.40
	0.10	1.13	1.47
	0.60	1.09	1.36
144	0.02	1.00	1.50
	0.10	1.00	1.55
	0.60	1.00	1.35

In this experiment, the unprotected exposure was observed with detectors above the circulating source. The protected exposure was obtained by inserting concrete slabs between source and detectors. In this arrangement, error due to lack of source reflection was eliminated since

the ground served as a reflector. The source was a cylinder which circulated so that the circular surface faced the dosimeters for a large portion of the travel. Since source anisotropy is usually most marked beyond the ends of the source, it is expected that this arrangement gave less error due to source anisotropy than the previously discussed experiment where a single source was placed on the ground or on the roof.

Because of the two above-mentioned reasons, and because the experiments were compared with calculations for Co-60 incident on concrete slabs, these experimental results were compared with existing theoretical calculations, no further calculations being carried out.

5 CONCLUSIONS

Various possible causes of error in comparing experiment with theory were considered in this investigation. The conclusions may be summarized as follows:

(1) Source anisotropy in free field measurements using a stationary source may cause an error on the order of 4% when normalizing the measured exposure to the calibrated source intensity. It must be emphasized that this is an approximate result only. If more accuracy in estimating this cause of error is required, more detailed calculations must be made for any particular experiment.

(2) The lack of reflector above a source in a roof experiment will cause larger error for a concrete than for a steel roof; this error for concrete will be of the order of 6% at 25 psf, 3% at 50 psf, and decreases to less than 1% above 100 psf. The source should have a reflector so as to include the equivalent of "skyshine" which is implicit in the moments theory calculations.

(3) Errors in the assumed value of thickness of a steel roof will cause an error in the calculated exposure of about 1% per inch thickness, for an error of 1% in assumed roof thickness.

(4) Comparison of the results of experiments with theoretical values often show agreement to within 10% when the geometry factor $L_a(\omega, X)$ is

used. There is a trend for the theory to predict lower values of exposure and reduction factor as solid angle decreases.

(5) It is recommended that the geometry factor $L_a(\omega,X)$ be used for roof penetration calculations in simple structures, and in that case an accuracy of greater than 10% in predicted reduction factor may often be expected.

REFERENCES

(1) Spencer, L. V.
"Structure Shielding Against Fallout Radiation from Nuclear Weapons," National Bureau of Standards, Monograph 42, June 1962.

(2) Eisenhauer, C.
"An Engineering Method for Calculating Protection Afforded by Structures Against Fallout Radiation," National Bureau of Standards, Monograph 76, 1964.

(3) Schmoke, M. A., and Rexroad, R. E.
"Attenuation of Simulated Fallout Radiation by the Roof of a Concrete Blockhouse," Nuclear Defense Laboratory, Army Chemical Center, Maryland, TR-6, August, 1961.

(4) Velletri, J. and McDonnell, C. H.
"An Experimental Evaluation of Roof Reduction Factors," Protective Structures Development Center, Fort Belvoir, Virginia, June, 1965 (Draft).

(5) Berger, M. J. and Doggett, J.
"Reflection and Transmission of Gamma Radiation by Barriers; Semi-analytic Monte Carlo Calculation," Journal of Research of the National Bureau of Standards, Volume 56, No. 2, February, 1956.

(6) Kirn, F. S., Kennedy, R. J., and Wyckoff, H. O.
Radiology, Volume 63, 94, 1954.

(7) Rexroad, R. E. and Schmoke, M. A.
"Scattered Radiation and Free Field Measurements from Distributed Co-60 and Cs-137 Sources," Nuclear Defense Laboratory, Army Chemical Center, Maryland, TR-2, September, 1960.

(8) Burson, Z. G. and Summers, R. L.
"Barrier Attenuation of Air-Scattered Gamma Radiation," CEX 63.3, June 18, 1965, U. S. A. E. C.

(9) Berger, M. J. and Raso, D. J.
"Backscattering of Gamma Rays," National Bureau of Standards, Report 5982, 1960.

(10) Berger, M. J. and Raso, D. J.
"Monte Carlo Calculations of Gamma Ray Backscattering," Radiation Research, Volume 12, 20-37, 1960.

(11) Price, B. T., Horton, C. C., and Spinney, K. T.
"Radiation Shielding," Pergamon Press, 1957.

REFERENCES Continued

(12) American Iron and Steel Institute
"Steel Products Manual," 1963.

(13) Grodstein, G. W.
"X-ray Attenuation Coefficients from 10 kev to 100 MeV," National Bureau of Standards, Circular 583, 1957.

(14) McGinnies, R. T.
"X-ray Attenuation Coefficients from 10 kev to 100 MeV - Supplement to National Bureau of Standards 583," 1959.

(15) Department of Defense, Office of Civil Defense
"Design and Review of Structures for Protection from Fallout Gamma Radiation," PM-100-1, February, 1965.

(16) Hubbell, J. H., Bach, R. L., and Lamkin, J. C.
"Radiation Field from a Rectangular Source," Journal of Research of the National Bureau of Standards, 64C, 2, April-June, 1960.

(17) Raso, D. J. and Woolf, S.
"The Dose Resulting from 1.25 MeV Plane Source behind Various Arrangements of Iron Barriers," Technical Operations Research Report No. TO-B 64-49, June 1964.

ACKNOWLEDGEMENT

The help and advice of Mr. C. Eisenhauer of the National Bureau of Standards, in carrying out the investigation reported here, is appreciated.

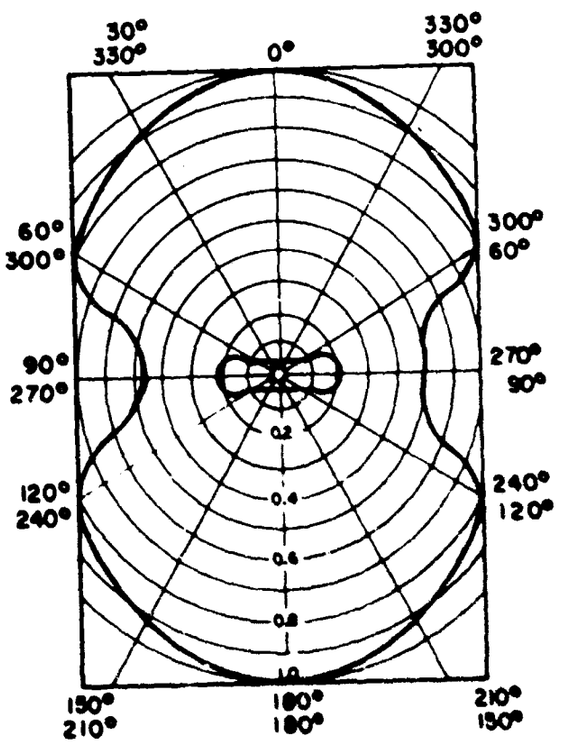

Fig. 1 - Relative directional calibration, cobalt-60 source.
From Burson and Summers (1968)

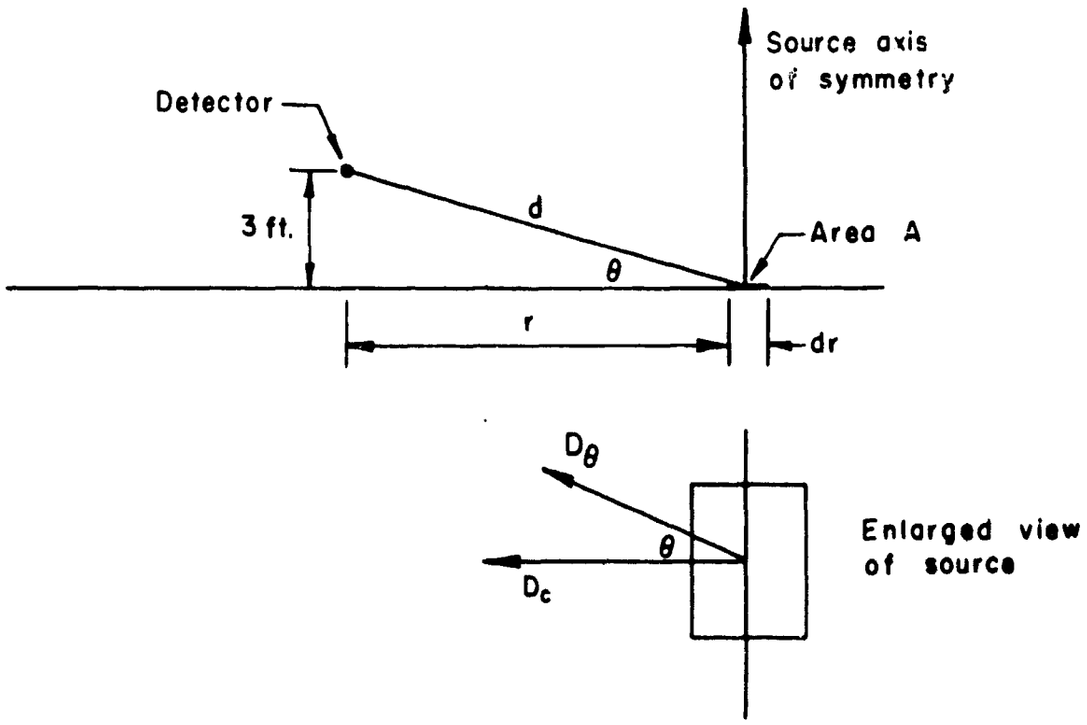

SCHEMATIC VIEW OF FREE FIELD EXPERIMENT AT THE NUCLEAR DEFENSE LABORATORY (REFERENCE 7)

FIG. 2

FIG. 3 ENERGY SPECTRUM OF 1 MeV PHOTONS REFLECTED FROM IRON

ISOTROPIC INCIDENCE, 1 MeV SOURCE
FROM TABLE A 19, BERGER & RASO
NBS 5982, 1960

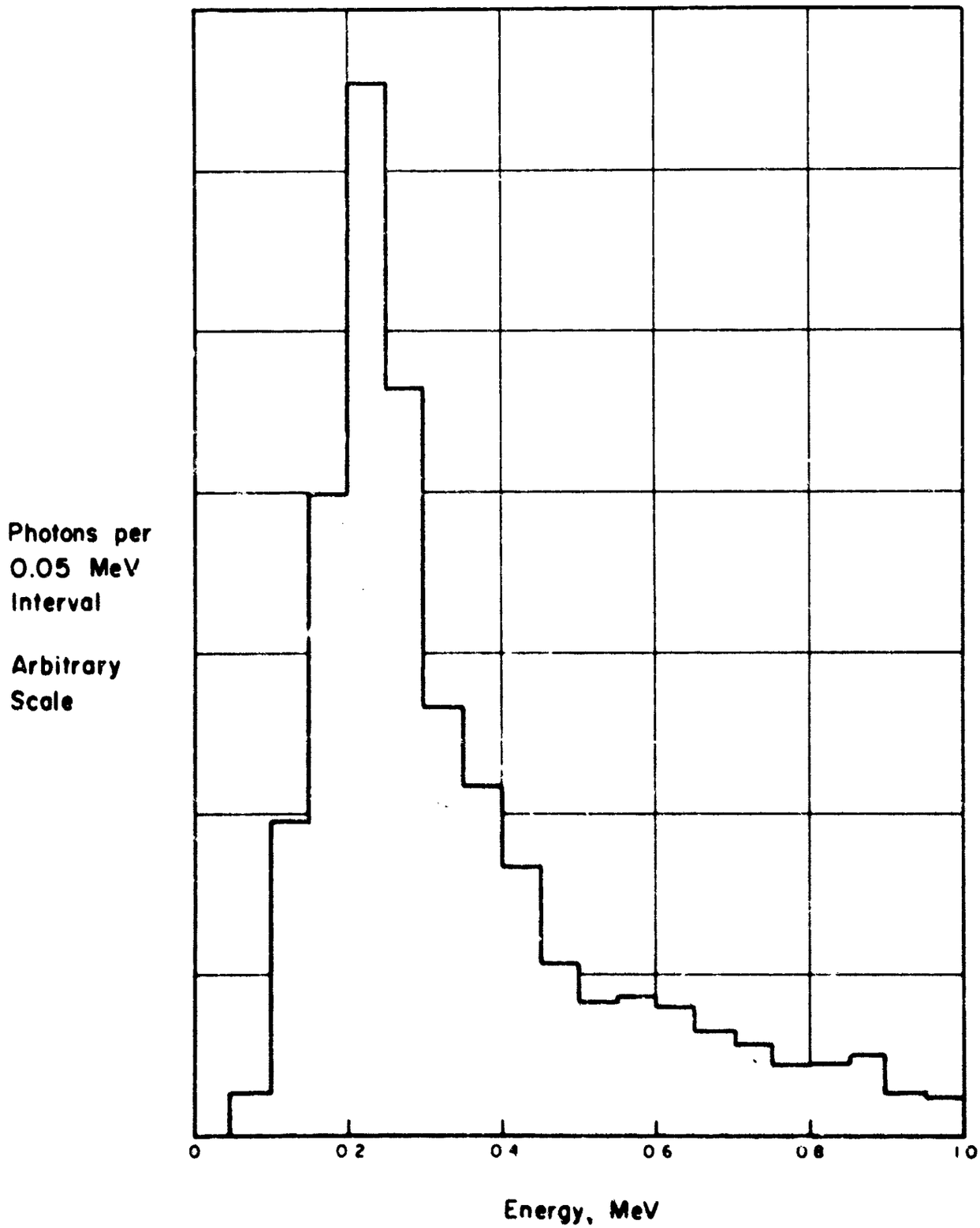

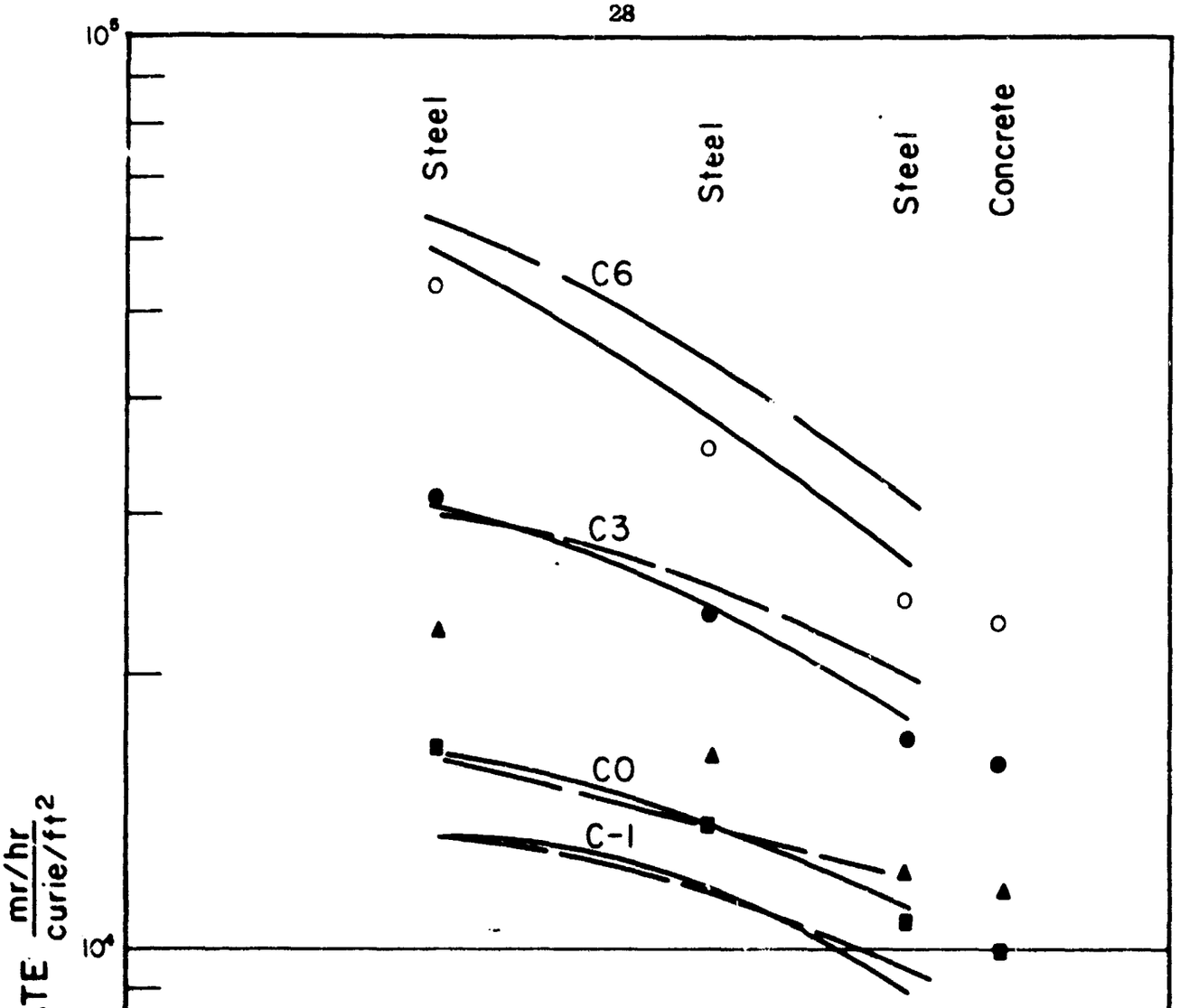

FIG.4 COMPARISON OF EXPERIMENTAL AND THEORETICAL EXPOSURE RATES

EXPERIMENTAL — SCHMOKE AND REXROAD 1962

○ Detector Position C6
● C3
▲ CO
■ C-1

Theoretical ——— $L_a(\omega, X)\, D(X)$

----- $L_c(\omega, X)\, D(X)$

Source Co-60

20 40 60

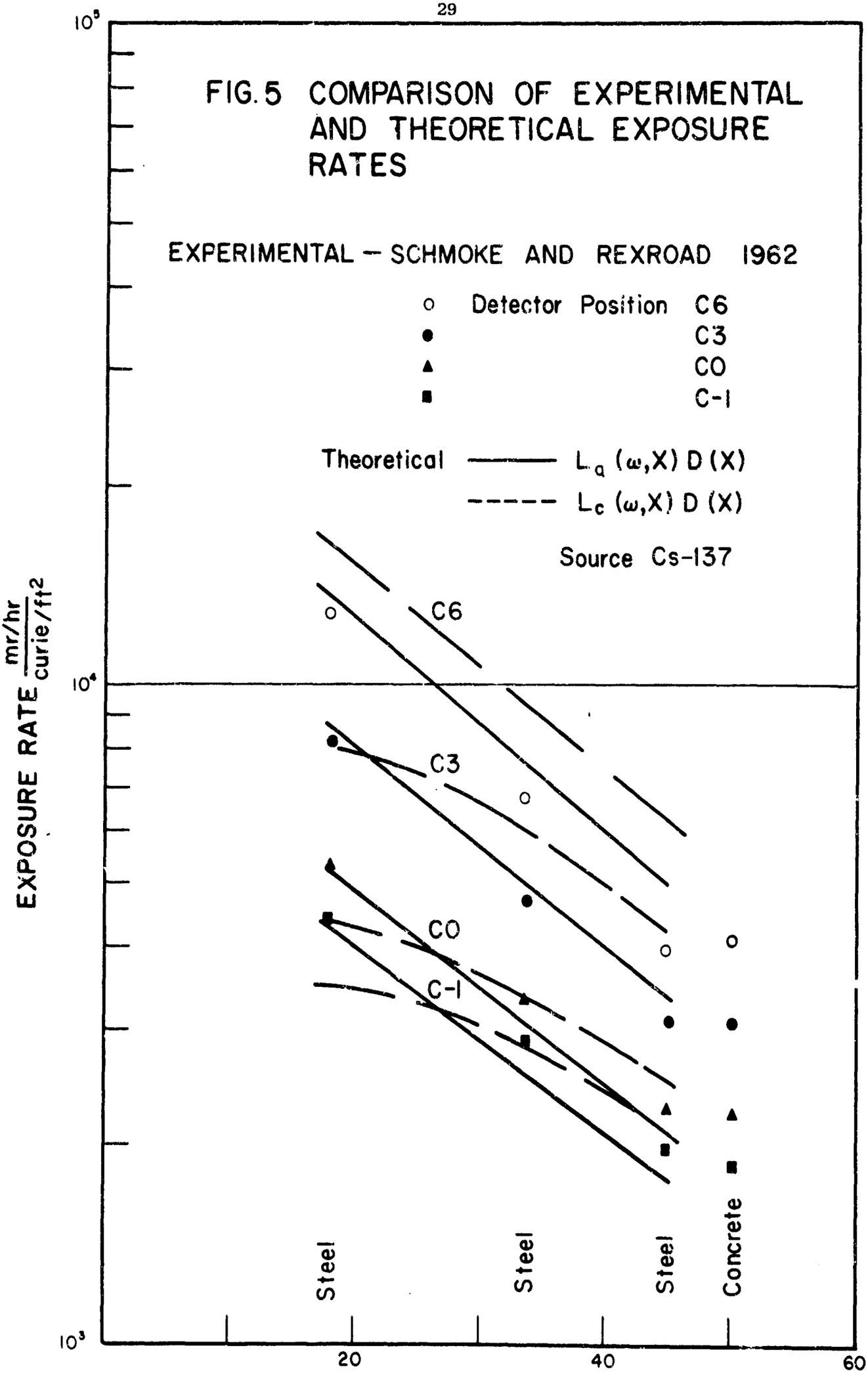
FIG. 5 COMPARISON OF EXPERIMENTAL AND THEORETICAL EXPOSURE RATES
EXPERIMENTAL – SCHMOKE AND REXROAD 1962
Detector Position C6
C3
C0
C-1
Theoretical $L_a(\omega,X)\,D(X)$
$L_c(\omega,X)\,D(X)$
Source Cs-137
EXPOSURE RATE $\frac{mr/hr}{curie/ft^2}$
10^5
10^4
10^3
C6
C3
C0
C-1
Steel
Steel
Steel
Concrete
20
40
60
BARRIER PSF

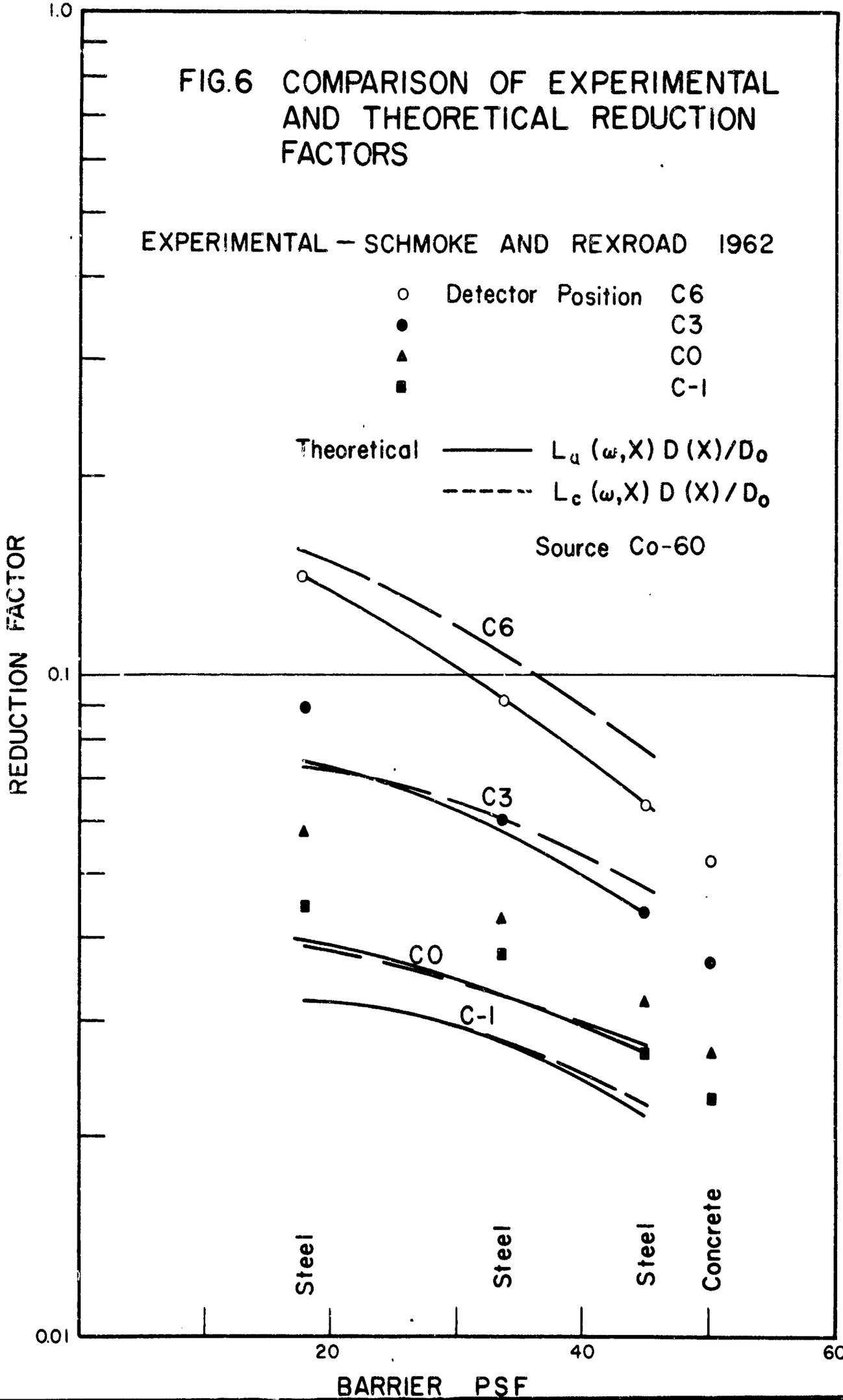
FIG.6 COMPARISON OF EXPERIMENTAL AND THEORETICAL REDUCTION FACTORS
EXPERIMENTAL – SCHMOKE AND REXROAD 1962
Detector Position C6
C3
C0
C-1
Theoretical $L_a(\omega,X)\,D(X)/D_o$
$L_c(\omega,X)\,D(X)/D_o$
Source Co-60
REDUCTION FACTOR
1.0
0.1
0.01
C6
C3
C0
C-1
Steel
Steel
Steel
Concrete
20
40
60
BARRIER PSF

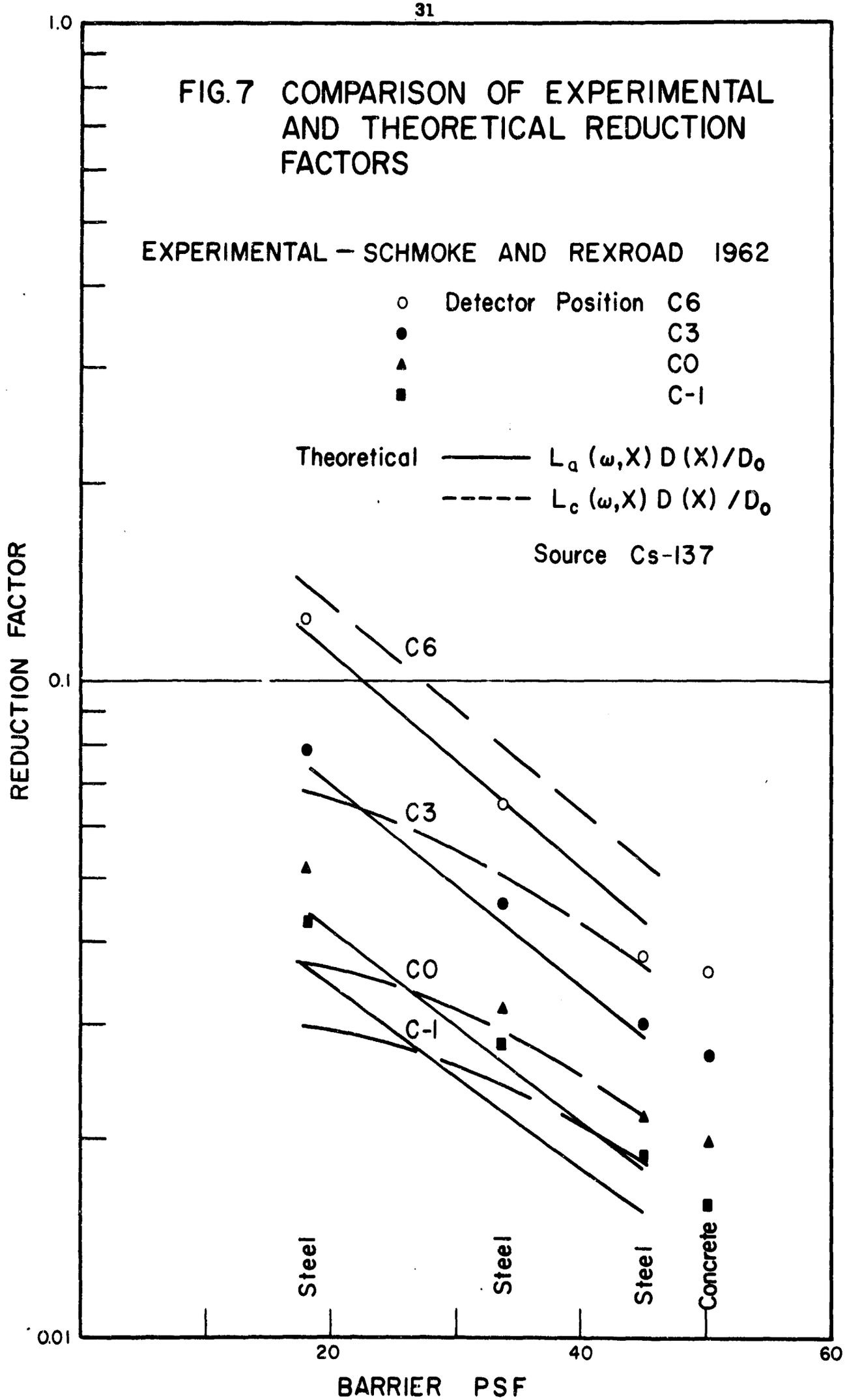
FIG. 7 COMPARISON OF EXPERIMENTAL AND THEORETICAL REDUCTION FACTORS
EXPERIMENTAL – SCHMOKE AND REXROAD 1962
Detector Position C6
C3
CO
C-1
Theoretical $L_a(\omega,X)\,D(X)/D_o$
$L_c(\omega,X)\,D(X)/D_o$
Source Cs-137
REDUCTION FACTOR
1.0
0.1
0.01
C6
C3
CO
C-1
Steel
Steel
Steel
Concrete
20
40
60
BARRIER PSF

APPENDIX A

CALCULATIONS OF EXPOSURE AND REDUCTION FACTOR DUE TO PLANE ISOTROPIC SOURCES IN IRON AND CONCRETE

Exposure distributions were calculated in infinite media of concrete, iron and air for plane isotropic sources, by the method of moments. Use was made of the code available at the National Bureau of Standards for this. Source energies were 1.33, 1.25, 1.17, 0.6616, 0.25, 0.10, and 0.05 MeV. The material cross sections were taken from those published by Grodstein[13] and McGinnies[14].

Table A1 gives the exposure in iron and in concrete at a number of depths for the various source energies. These values are plotted in Figures A1 to A4.

Table A2 shows the following quantities for each of five source energies; the exposure in air three feet from the source plane in MeV/gm per photon/cm^2, and the ratio of scattered to total exposure at the detector.

Conversion from MeV/gm per photon/cm^2 to roentgen/hr per curie/ft^2 is shown in Section 4.1. Reduction factors may be obtained by dividing the exposures in concrete or iron by the exposure in air three feet from the source plane at the relevant source energy.

It should be noted that the exposures are given as functions of the mass thickness Z. This is not to be confused with the equivalent mass thickness X of NBS 42[1].

TABLE A1

Exposures in MeV/gm per photon/cm^2 for Iron and Concrete at Different Source Energies and Depths

E_o MeV	$\mu_o z$	Iron		Concrete	
		z psf	Exposure	z psf	Exposure
1.33	0.5	19.9	0.0185	18.6	0.0199
	1.0	39.7	0.00932	37.1	0.0103
	1.5	59.6	0.00520	55.7	0.00588
	2.0	79.5	0.00302	74.2	0.00347
	2.5	99.3	0.00179	92.8	0.00209
	3.0	119	0.00107	111	0.00127
	4.0	159	0.000395	148	0.000473
	8.0	318	0.00000779	297	0.00000769
1.25	0.5	19.3	0.0178	18.0	0.0193
	1.0	38.5	0.00901	35.9	0.0101
	1.5	57.8	0.00504	53.9	0.00575
	2.0	77.0	0.00293	71.9	0 00340
	2.5	96.3	0.00174	89.4	0.00205
	3.0	116	0.00105	108	0.00125
	4.0	154	0.000387	144	0.000469
	8.0	308	0.00000771	288	0.00000973
1.17	0.5	18.6	0.0171	17.4	0.0186
	1.0	37.2	0.00867	34.8	0.00973
	1.5	55.9	0.00486	52.2	0.00559
	2.0	74.5	0.00284	69.5	0.00332
	2.5	93.1	0.00169	86.9	0.00201
	3.0	112	0.00102	104	0.00123
	4.0	149	0.000376	139	0.000463
	8.0	298	0.00000759	278	0.00000977
.6616	0.5	14.1	0.0113	13.3	0.0130
	1.0	28.2	0.00583	26.5	0.00709
	1.5	42.2	0.00332	39.8	0.00421
	2.0	56.3	0.00197	53.0	0.00258
	2.5	70.4	0.00119	66.3	0.00160
	3.0	84.4	0.000723	79.5	0.00100
	4.0	113	0.000274	106	0.000395
	8.0	225	0.00000597	212	0.00000961

TABLE A1 (Continued)

E_o MeV	$\mu_o z$	Iron		Concrete	
		z psf	Exposure	z psf	Exposure
0.25	0.5	8.66	0.00400	8.93	0.00584
	1.0	17.3	0.00200	17.9	0.00335
	1.5	26.0	0.00111	26.8	0.00206
	2.0	34.7	0.000636	35.7	0.00130
	2.5	43.3	0.000374	44.6	0.000822
	3.0	52.0	0.000223	53.6	0.000525
	4.0	69.3	0.0000806	71.4	0.000215
	8.0	139	0.00000155	143	0.00000588
0.10	0.5	3.00	0.000901	6.03	0.00193
	1.0	5.99	0.000389	12.1	0.00105
	1.5	8.99	0.000189	18.1	0.000613
	2.0	12.0	0.0000978	24.1	0.000366
	2.5	15.0	0.0000522	30.1	0.000221
	3.0	18.0	0.0000286	36.2	0.000135
	4.0	24.0	0.00000893	48.2	0.0000507
	8.0	47.9	0.000000110	96.4	0.00000108
0.05	0.5	0.569	0.000577	2.92	0.000972
	1.0	1.14	0.000232	5.84	0.000448
	1.5	1.71	0.000107	8.76	0.000228
	2.0	2.28	0.0000530	11.7	0.000121
	2.5	2.85	0.0000273	14.6	0.0000665
	3.0	3.42	0.0000144	17.5	0.0000371
	4.0	4.55	0.00000425	23.4	0.0000120
	8.0	9.11	0.0000000443	46.7	0.000000163

TABLE A2

Exposures in Air Three Feet from a Plane Isotropic Source

E_o MeV	Exposure MeV/gm per photon/cm^2	Ratio $\frac{\text{Scattered Exposure}}{\text{Total Exposure}}$
1.33	0.0957	0.172
1.25	0.0911	0.177
1.17	0.0865	0.181
0.6616	0.0530	0.231
0.05	0.00624	0.503

From the above table, it can be calculated that:

For Co-60, exposure rate three feet above source plane = 482 roentgen/hr per curie/ft^2 ;

For Cs-137, exposure rate three feet above source plane = 118 roentgen/hr per curie/ft^2 .

The assumed density of air = 0.001205 g/cc .

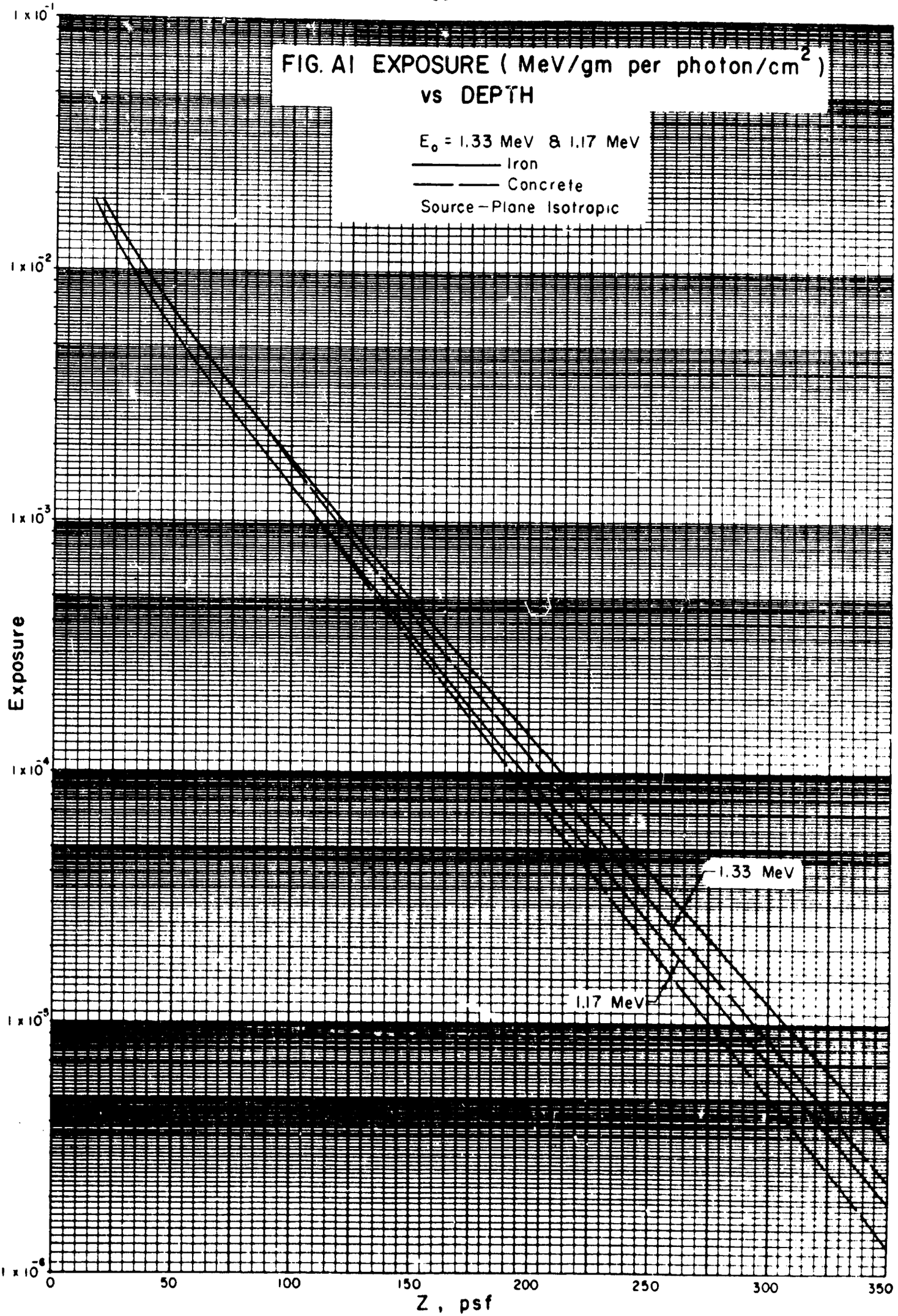
FIG. A1 EXPOSURE (MeV/gm per photon/cm^2) vs DEPTH
E_o = 1.33 MeV & 1.17 MeV
Iron
Concrete
Source – Plane Isotropic
1.33 MeV
1.17 MeV
Exposure
1×10^{-1}
1×10^{-2}
1×10^{-3}
1×10^{-4}
1×10^{-5}
1×10^{-6}
0
50
100
150
200
250
300
350
Z , psf

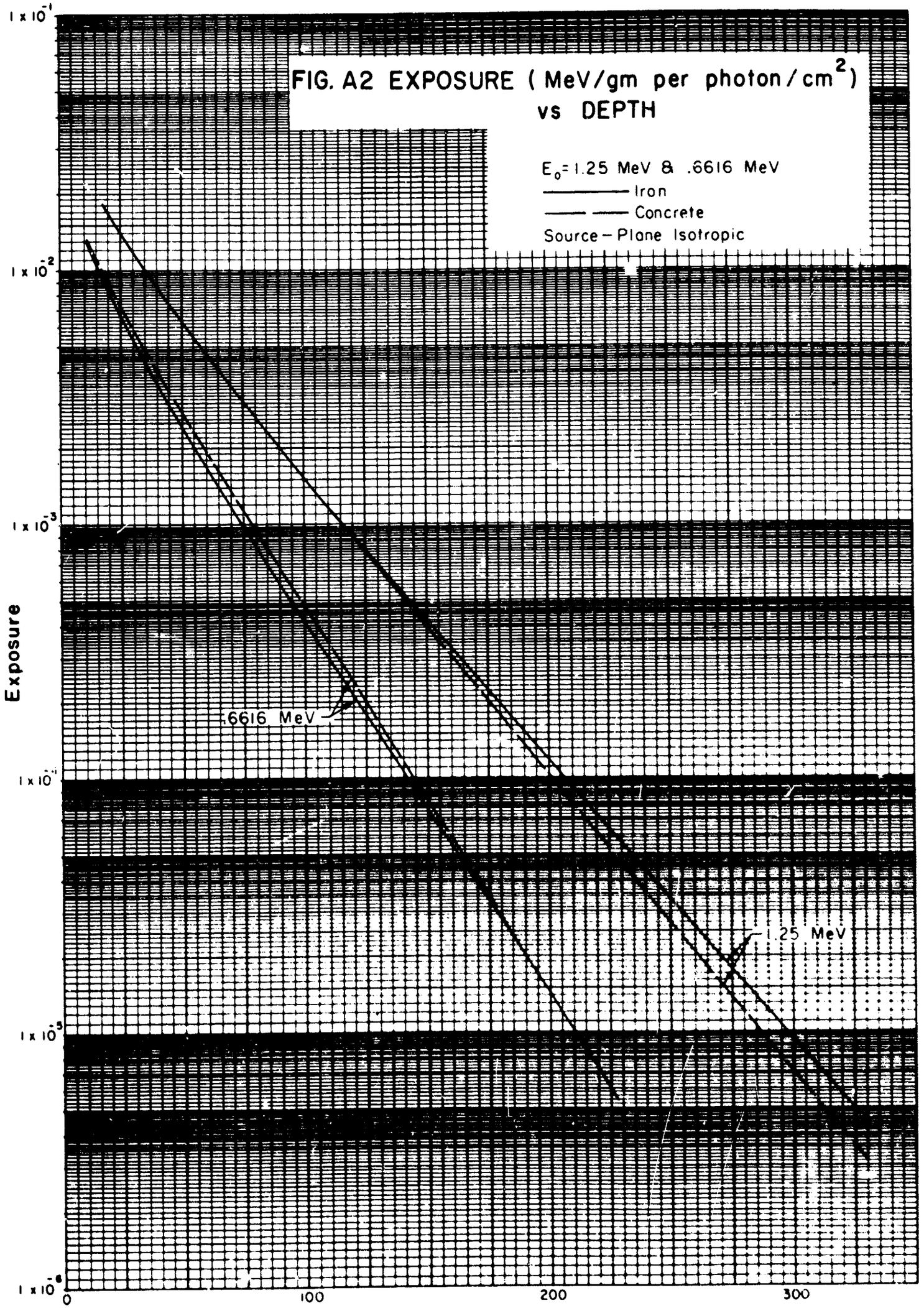
FIG. A2 EXPOSURE (MeV/gm per photon/cm^2) vs DEPTH
E_0 = 1.25 MeV & .6616 MeV
Iron
Concrete
Source – Plane Isotropic
Exposure
1 x 10^{-1}
1 x 10^{-2}
1 x 10^{-3}
1 x 10^{-4}
1 x 10^{-5}
1 x 10^{-6}
.6616 MeV
1.25 MeV
0
100
200
300

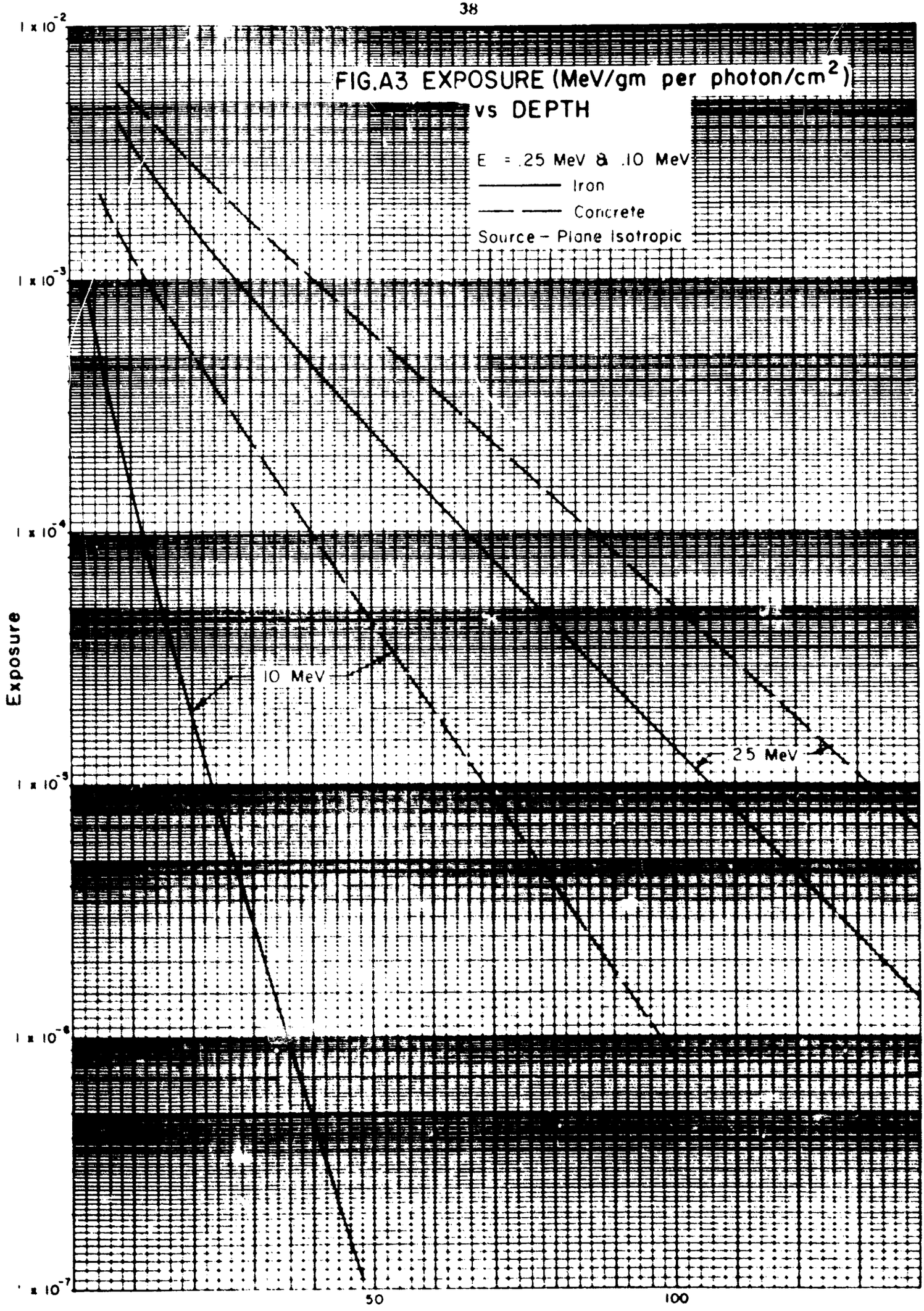
FIG.A3 EXPOSURE (MeV/gm per photon/cm²) vs DEPTH
E = .25 MeV & .10 MeV
Iron
Concrete
Source – Plane Isotropic
Exposure
1 x 10⁻²
1 x 10⁻³
1 x 10⁻⁴
1 x 10⁻⁵
1 x 10⁻⁶
1 x 10⁻⁷
10 MeV
25 MeV
50
100
Z, psf

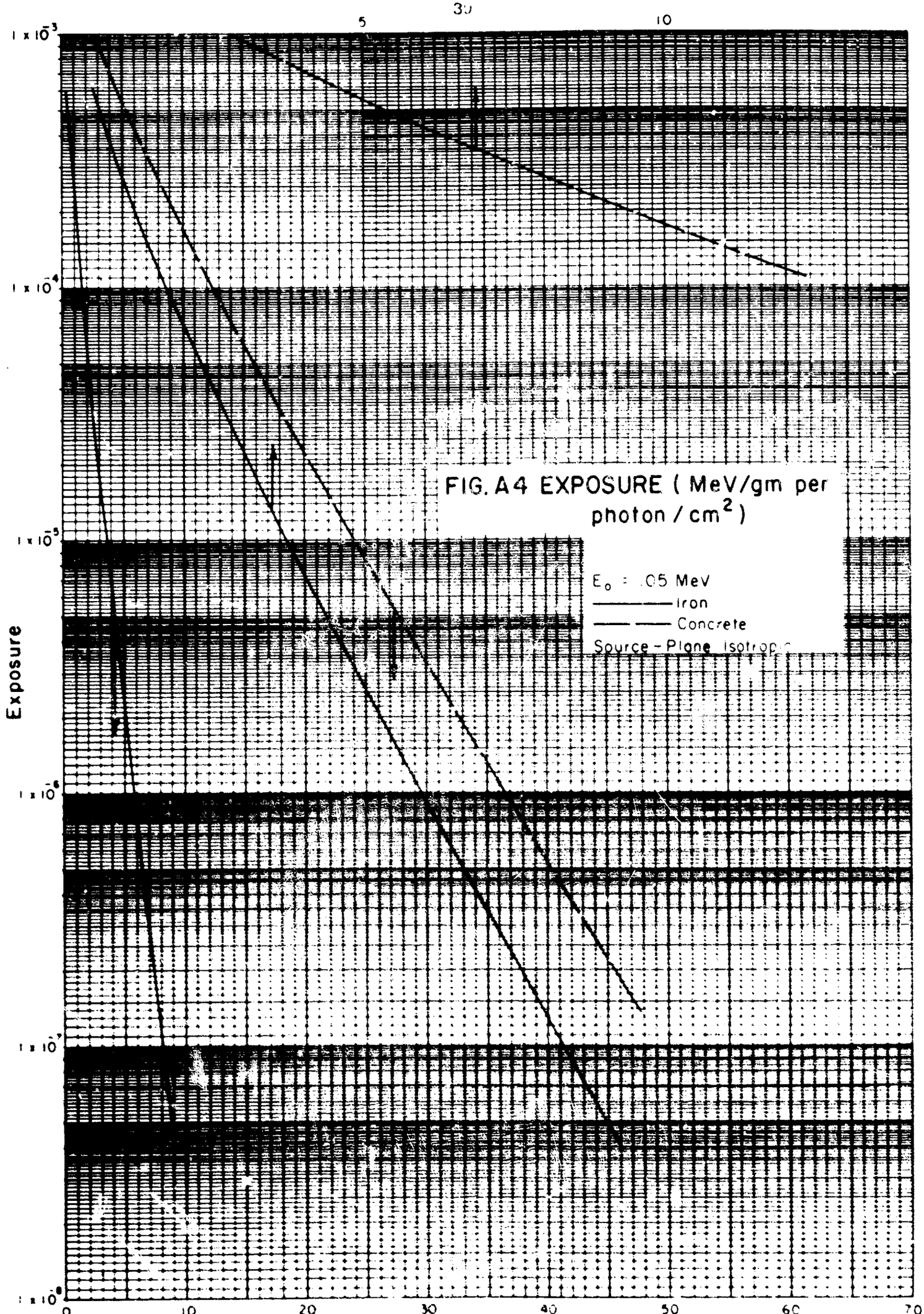
5
10
1 x 10⁻³
1 x 10⁻⁴
1 x 10⁻⁵
1 x 10⁻⁶
1 x 10⁻⁷
1 x 10⁻⁸
Exposure
0
10
20
30
40
50
60
70
FIG. A4 EXPOSURE (MeV/gm per photon / cm²)
E₀ = .05 MeV
Iron
Concrete
Source - Plane Isotropic

APPENDIX B

A REVIEW OF GROUND CONTRIBUTION TO FALLOUT RADIATION PENETRATION THROUGH SIMPLE STRUCTURES

B.1 Introduction

There has been a flurry of experimental efforts in the past few years to check the validity of the functions used in computing the ground contamination contribution to fallout radiation penetration into simple structures, under infinite field conditions. In many cases, it is difficult to design experiments which will isolate the function to be studied; and therefore the results obtained do not always lead to unambiguous conclusions. It is believed appropriate at this time to review some of the basic technology and the conceptual basis therefor. This will provide an insight into the validity of previous experimental programs and will be a basis for recommendations as to the directions for fruitful research in the near future.

Let us consider the basic formula presently used to calculate the ground contribution to the attenuation function of a simple, rectangular-one-story structure under infinite fallout field conditions:

$$R = B_w \left\{ C_d E_d (1 - S_w) + C_s E_s S_w \right\} \quad . \qquad (1)$$

The notation used is roughly similar to that in the OCD Engineering Manual[15] and should be readily identified by anyone familiar with the Manual.*

We will attempt to explain this formula in terms of "operational" concepts, that is, in terms of experiments (perhaps idealized) devised to measure them. Concepts which cannot be explained in such a manner

---

*This is essentially the same as the formula for C_f given in Example 4-3 of the Engineering Manual[15]. Our terms C_d and C_s are actually split into two terms in the Manual. Our term E_d does not appear in the Manual formula, but this is explained below. The remaining correspondence of terms is obvious.

cannot be determined experimentally. The various terms in the formula can be related to ratios of exposure rate measurements carried out for various structural configurations. These are depicted in Figure B-1 and are discussed below.

B.2 Explanation of Situations Depicted

Before discussing the interrelationships of these configurations, or "situations," presented, it is desirable to describe them and to indicate the present theoretical (mathematical) approach to finding the exposure rates in the designated detector locations. The formulations are taken or inferred from Eisenhauer's NBS Monograph 76[2], with further reference as necessary to Spencer's NBS Monograph 42[1]. (These will hereinafter be called NBS-76 and -42, respectively.)

Situation 1 is the reference situation. It established the exposure rate

$$D_1 = \int_{-1}^{1} \ell(3', \cos\theta) \; d(\cos\theta) \quad , \tag{2}$$

in terms of the ℓ-function defined in NBS-42. This formula is exact, and in fact the ℓ-function is normalized so as to make D_1 equal to unity.

Situation 2 provides an exposure rate behind two walls, very close together. The walls are of indefinite height and length, because the detector is so close to the walls that radiation can be assumed to be entering the detector from all directions (4π steradians). The wall mass thickness is the same as that of the given blockhouse structure. The exposure rate in this situation is based on the NBS-42 function for penetration through a single wall (Eq. 27.7):

$$W(X,H) = \int_0^1 d(\cos\theta) \cos\theta \; s(X, \cos\theta) \times (1/2\pi) \int_0^{2\pi} d\varphi \; \ell(H, \sin\theta \cos\varphi) \quad . \tag{3}$$

This function must be multiplied by 2, to account for contribution through two walls rather than one. The result is then slightly too high for small values of the mass thickness, X, because the function W always includes the effect of an infinitely thick backscatterer behind the detector instead of a finite wall. NBS-76 indicates that this can be allowed for by deliberately lowering the plotted curves for small X , so that the resulting exposure rate is unity for X = 0 and H = 3 feet . Thus,

$$D_2 = 2W(X,H) \qquad (4)$$

for all but very small values of X . However, there are some minor approximations inherent in the above formula for W , so that Equation (4) is not rigorously correct, even for very large values of X . (See NBS-42, p. 30)

Situation 2-0 is the same as Situation 2, except that the mass thickness of the walls is zero. The detector response is the same as it would be in the open, that is,

$$D_{2-0} = \int_{-1}^{1} \ell(H,\cos\theta)\, d(\cos\theta) = L(H) \qquad (5)$$

where the ℓ-function is defined in NBS-42 (Equation 27.2). D_{2-0} obviously equals D_1 when H equals three feet.

Situation 2-∞ is also similar to Situation 2, except that the mass thickness of the walls is approaching infinity. This is to be regarded as being brought about by maintaining the actual thickness but letting the density approach infinity. In comparison with the value of D_2, D_{2-0} is negligible. However, for the sake of comparison with exposure rate for other configurations having walls of mass thickness approaching infinity, one must consider in the limit the variation, with respect to direction, of the differential contribution of radiation entering the detector. The situation is one which is extremely difficult to establish experimentally, but there are theoretical means of obtaining radiation data at very great penetration depths; and, since the angular and energy distribution of the radiation field tends to seek an approximate equilibrium at great depths, there is reason to expect that a description of $D_{2-\infty}$ can be obtained in such a way. The primary information needed is

the directional distribution of radiation emitted from the wall, or - looking at the matter from the detector point of view - the directional distribution of differential exposure contributions at the detector. NBS-76 implicitly assumes that the directional density function depicting the radiation emitted from the walls is separable into components dependent on vertical (polar) and horizontal (azimuthal) angles, respectively. Thus, this function is assumed to have the form:

$$F(\cos\theta,\varphi) = p(\varphi)\, q(\cos\theta) \ , \tag{6}$$

where θ and φ are the polar and azimuthal angles, respectively relative to a frame of reference with a vertical polar axis. If the azimuthal angle is measured relative to a line normal to a wall, then NBS-76 gives as an expression for $p(\varphi)$, based upon an assumed cosine distribution,

$$p(\varphi) = \frac{\cos\varphi}{2} \ . \tag{7}$$

The exposure rate is given by integration of $F(\cos\theta,\varphi)$ over all directions, thus:

$$D_{2-\infty} = 2 \int_{-\pi/2}^{\pi/2} \frac{\cos\varphi}{2}\, d\varphi \int_{-1}^{1} q(\cos\theta)\, d(\cos\theta) \tag{8}$$

$$= 2 \int_{-1}^{1} q(\cos\theta)\, d(\cos\theta) \ . \tag{9}$$

It is to be noted that the adequacy of the assumption as to separability of the function $F(\theta,\varphi)$ has never been studied; and, even if it is approximately separable, the accuracy of the cosine assumption for $p(\varphi)$ has not been verified.

Situation 3-0 involves a circular structure of zero mass thickness; and thus D_{3-0} is the exposure rate above an infinite contaminated plane, on the axis of a decontaminated circle which subtends the same solid angle at the detector position as does the rectangular base of the structure under consideration. A general formula for the exposure rate can be expressed as:

$$D_{3-0} = 1/2\pi \int \ell(H,\cos\theta)\, d\Omega \quad , \tag{10}$$

where the integration is over the solid angle subtended at the detector by the walls. Through the cylindrical symmetry of the situation, this becomes:

$$D_{3-0} = \int_{-\cos\theta_\mu}^{0} \ell(H,\cos\theta)\, d(\cos\theta) + \int_{0}^{\cos\theta_\ell} \ell(H,\cos\theta)\, d(\cos\theta) \tag{11}$$

$$= \int_{-\cos\theta_\mu}^{\cos\theta_\ell} \ell(H,\cos\theta)\, d(\cos\theta) \quad . \tag{12}$$

This formulation is not exact in principle, since the ℓ-function is for a completely contaminated plane and a collimated detector, while this case is for a partially cleared plane and a completely uncollimated detector. The degree of approximation is quite close, however, in most practical cases.

Situation 3-∞ has a rectangular plan similar to that of the structure itself, but it is considered of infinite extent in the vertical direction. The mass thickness approaches infinity. The statements relative to Situation 2-∞ apply in general here also. Under the same assumptions, the exposure rate is found to be:

$$D_{3-\infty} = 2 \int_{-1}^{1} q(\cos\theta)\, d(\cos\theta) \left[\int_{0}^{\varphi_a} \cos\varphi\, d\varphi + \int_{0}^{\frac{\pi}{2} - \varphi_a} \cos\varphi\, d\varphi \right] \tag{13}$$

$$= 2(\sin\varphi_a + \cos\varphi_a) \int_{-1}^{1} q(\cos\theta)\, d(\cos\theta) \quad . \tag{14}$$

Situation 3'-∞ is similar to Situation 3-∞, except that the plan is circular instead of rectangular. The circle has the same area as that

specified for Situation 3-0. NBS-76 makes the same assumption of separability of vertical and horizontal dependence, and in this case an additional assumption is made that the vertical dependence is similar to that of the skyshine portion of the ℓ-function, that is:

$$q(\cos\theta) = k \cdot \ell(3', -|\cos\theta|) \quad , \tag{15}$$

where k is an appropriate constant. The dependence on the negative of the absolute value of $\cos\theta$ shows that the contribution from above and below the detector plane is believed to be symmetric at deep penetrations. (One should note that here, just as in Situation 3-∞, the wall is effectively of infinite depth as well as infinite height.) For this case any line from the detector is perpendicular to the wall, and thus from Equation (7), $p(\varphi)$ equals $1/2$ at the detector position. Then

$$D_{3'-\infty} = \int_0^{2\pi} \frac{d\varphi}{2} \cdot 2k \int_{-1}^{0} \ell(3', \cos\theta)\, d(\cos\theta) \tag{16}$$

$$= 2\pi k \int_{-1}^{0} \ell(3', \cos\theta)\, d(\cos\theta) \tag{17}$$

$$= 2\pi k\, S(3') \quad , \tag{18}$$

where S is a function defined in NBS-42 (Equation 27.3).

Situation 4-0 differs from Situation 3-0 only in that the cleared area within the "phantom" structure is rectangular rather than circular, being similar in plan to the structure under consideration. A general formula for the exposure rate is given by

$$D_{4-0} = \frac{1}{2\pi} \int \ell(H, \cos\theta)\, d\Omega \quad , \tag{19}$$

where the integration is over the solid angle subtended at the detector by the walls of the structure. The technology as established[15] assumes the identity of D_{3-0} and D_{4-0}, although NBS-76 notes that in principle this is not true. Calculation of D_{4-0} can be made, although it is tedious because the limits of integration are not simple functions of the polar coordinates which are suitable for the ℓ-function.

Situation 4-∞ is the situation for a finite-sized building of rectangular plan. It is the same shape as the structure under investigation, but it has walls of infinite density. The angular distribution of detector response in such case has not been previously defined, but in principle it can be obtained by theoretical means, if one can show that deep penetrating radiation approaches an equilibrium directional distribution. In terms of the function $F(\cos,\varphi)$ introduced in the discussion of Situation 2-∞ , the exposure rate is simply given by:

$$D_{4-\infty} = \int F(\cos\theta,\varphi)\, d\Omega \quad , \tag{20}$$

where the integration is over all solid angle subtended by the walls at the detector.

Situation 4'-∞ is similar to that in Situation 3'-∞ , except that the upper and lower limits on the wall are finite. Thus we would have, according to the distribution assumed by NBS-76:

$$D_{4'-\infty} = \pi k \left\{ \int_{-\cos\theta_\ell}^{0} \ell(3', \cos\theta)\, d(\cos\theta) + \int_{-\cos\theta_\mu}^{0} \ell(3',\cos\theta)\, d(\cos\theta) \right\} \tag{21}$$

$$= \pi k \left[G(1-\cos\theta_\ell) + G(1-\cos\theta_\mu) \right] \quad , \tag{22}$$

where G is defined in NBS-76 (Section 4.4, line 25). The validity of this equation is based on several assumptions as noted for Situations 3-∞ and 3'-∞ .

Situation 4 is the real structure, of finite dimensions, actual wall density, and rectangular shape. The exposure rate is expressible as an integral over all directions subtended by the walls at the detector of the directionally differential detector response function, but this

definition, though obvious, is not directly useful. A direct and exact calculation is not easily done; and it would require an elaborate Monte Carlo type of computation not suited for engineering purposes.

B.3 Discussion and Conclusions

Since R is defined as D_4/D_1, the value of R may be established in terms of the exposure rates for the various situations already discussed, according to the following analysis:

$$R = \frac{D_4}{D_1} = \frac{D_2}{D_1} \cdot \frac{D_4}{D_2} \quad . \tag{23}$$

One may consider that the ratio D_4/D_2, which involves true wall mass thicknesses, can be interpolated between the corresponding ratios for infinite and zero mass wall thicknesses, respectively, that is, $D_{4-\infty}/D_{2-\infty}$ and D_{4-0}/D_{2-0}. The interpolation factor is called S_w, and thus

$$\frac{D_4}{D_2} = S_w \left(\frac{D_{4-\infty}}{D_{2-\infty}} \right) + (1-S_w) \left(\frac{D_{4-0}}{D_{2-0}} \right) \quad . \tag{24}$$

NBS-76 assumes that

$$S_w = \frac{B_p(X)-1}{B_p(X)} \quad , \tag{25}$$

where B_p is the buildup factor for cobalt-60 normally incident on concrete (or similar material). Such assumption involves two separate hypotheses: (1) the only significant parameter affecting the value of S_w is the actual mass thickness of the structural walls; (2) the dependence is given by the ratio of scattered to uncollided cobalt-60 radiation which can penetrate the walls.

Thus, one obtains, following this approach:

$$R = \frac{D_2}{D_1} \left\{ S_w \left(\frac{D_{4-\infty}}{D_{2-\infty}} \right) + (1-S_w) \left(\frac{D_{4-0}}{D_{2-0}} \right) \right\} \tag{26}$$

$$= \frac{D_2}{D_1}\left\{ S_w \left(\frac{D_{4-\infty}}{D_{3-\infty}} \right)\left(\frac{D_{3-\infty}}{D_{2-\infty}} \right) + (1-S_w) \left(\frac{D_{4-0}}{D_{3-0}} \right)\left(\frac{D_{3-0}}{D_{2-0}} \right) \right\} \quad (27)$$

If the assumption is made that

$$\frac{D_{4-\infty}}{D_{3-\infty}} = \frac{D_{4'-\infty}}{D_{3'-\infty}} \quad , \quad (28)$$

which involves some degree of approximation, however close, then Equation (1) follows, through the establishment of the following definitions:

$$B_w = \frac{D_2}{D_1} \quad (29)$$

$$G_s = \frac{D_{4'-\infty}}{D_{3'-\infty}} \quad (30)$$

$$G_d = \frac{D_{3-0}}{D_{2-0}} \quad (31)$$

$$E_s = \frac{D_{3-\infty}}{D_{2-\infty}} \quad (32)$$

$$E_d = \frac{D_{4-0}}{D_{3-0}} \quad (33)$$

The mathematical descriptions of these concepts follow from the definitions. Since D_1 is unity, B_w is obtained by the same formulation as D_2 (see Equation 3 and 4 and associated text). G_s becomes, from Equations (18) and (22),

$$G_s = \frac{\left[G(1-\cos\theta_\ell) + G(1-\cos\theta_\mu) \right]}{2\, S(3')} \quad (34)$$

$$\approx 5 \left[G(1-\cos\theta_\ell) + G(1-\cos\theta_\ell) \right] \quad , \quad (35)$$

since $S(3')$ is approximately equal to 0.1 . From Equations (5) and (12), one obtains:

$$G_d = \frac{\int_{-\cos\theta_\mu}^{\cos\theta_\ell} \ell(H,\cos\theta)\, d(\cos\theta)}{L(H)} \quad , \tag{36}$$

From Equations (9) and (14), one derives:

$$E_s = \sin\varphi_a + \cos\varphi_a \quad . \tag{37}$$

From Equations (10) and (19), we see:

$$E_d = \frac{\int_{\text{rect.}} \ell(H,\cos\theta)\, d\Omega}{\int_{\text{cyl.}} \ell(H,\cos\theta)\, d\Omega} \tag{38}$$

where the integrations are over the solid angle subtended at the detector by the walls for the rectangular and equivalent cylindrical situations, as indicated. NBS-76 (Section 4.5) suggests that this ratio can be obtained from the work of Hubbell et al.[16]. Although the situations considered by Hubbell differed slightly from those involved here, the results so obtained would probably be a close approximation. Present engineering practice[15], however, is to assume this value to be unity.

It is to be noted that the concepts involving essentially infinitely thick structures, G_s and E_s, involve situations which are probably impossible to reproduce experimentally. Independent determinations of these so-called "non-wall scattered" factors[15], or even their product, by experimental means seem out of the question. Indirect experimental determination of these factors by measuring the overall reduction factor cannot be achieved unless all the other factors in Equation (1) are accurately known and the various assumptions inherent in the development of that formula have been justified.

The important assumptions and approximations which are subject to verification or possible improvement are:

(a) That deeply penetrating radiation can be split into factors depending separately upon vertical and azimuthal angles.

(b) That the azimuthal variation for deeply penetrating radiation follows a cosine distribution.

(c) That the vertical variation for deeply penetrating radiation is approximated by the skyshine portion of the ℓ-function.

(d) That the shape factor E_d is always very near unity.

(e) That the interpolation factor S_w is dependent only on wall mass thickness and that it is approximately given by the formula presented as Equation (25).

(f) That G_s as determined on the basis of cylindrical structure situations are valid for rectangular structures.

One might ask at this point whether it is worth seriously considering abandoning the whole approach to ground contribution to structure penetration typified by Equation (1). However, it must be observed that the present formulation has been shown by many experiments to be rather successful thus far and is now deeply ingrained into the minds of many fallout shelter analysts. The edifice thus appears to require bolstering rather than replacement.*

B.4 Recommendations

It is recommended that if further work on ground penetration into blockhouses be undertaken, it be directed along the following lines in the immediate future:

(a) Make further efforts to pin down B_w for all practical thicknesses, either experimentally or theoretically or both, so as to give confidence in definitive results drawn from such work within an uncertainty on the order of perhaps 10% .

(b) Do further work, either experimentally or theoretically or both, to obtain or improve values of G_d and E_d for "phantom" buildings (i. e., those of zero wall mass thickness), to the same order of accuracy as indicated above.

---

*C. Eisenhauer disagrees with this (personal communication). He would prefer a completely fresh approach, avoiding the S_w interpolation procedure.

(c) Determine E_s and G_s (or their product if they are not separable) by approved theoretical techniques, to within the same order of accuracy as above.

(d) After the above factors are known with reasonable accuracy, resume experimental blockhouse work to look for the best values of S_w and to determine the effect of various parameter changes on it. This could possibly be supplemented with Monte Carlo calculations using the actual blockhouse configurations. If the other functions are known within an uncertainty of about 10% , one should be able to determine S_w to within about 20% .

It is not implied that previous experimental work in these matters has been wasted. However, it is believed that after items (a), (b), and (c) have been accomplished, previous work could be re-interpreted in the light of this approach, along with further work mentioned in subparagraph (d).

Some justification for continuation of work on this basic, elementary problem appears to be necessary, especially in view of the apparant adequacy of the approach for simple geometries, as indicated above. Such justification arises most strongly from the fact that a great many of the problems involving more complicated type of structures and source distributions are solved by methods which spring from this basic method and assume its adequacy. It is well known that there are serious discrepancies between experimental values and engineering predictions in connection with many of these complex situations, such as the blockhouse basement problem ("in-and-down"), the protection prediction for upper floors of multistory structures ("in-and-up"), the mutual shielding problem ("finite source plane"), and others. In order to solve these difficult problems in fallout shielding methodology, the logical framework of the more basic part of the technology must be sufficiently firm to assure that the troubles in more complex situations do not stem, even in part, from these shaky foundations. Therefore, more careful attention in research should be devoted to strengthening the fundamentals of the present fallout shielding technology.

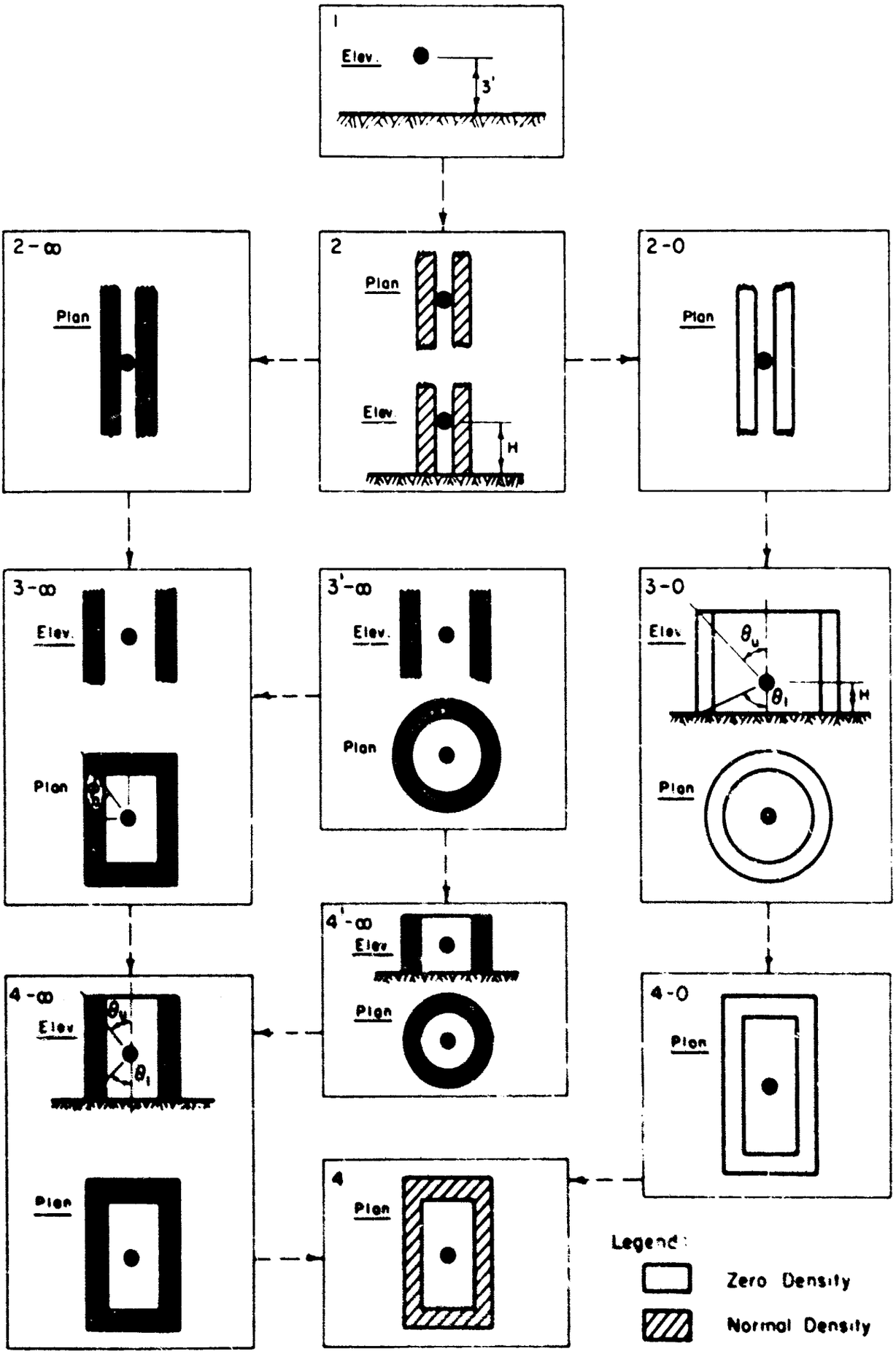

Figure 61. Schematic Order of Situations Involved in Analysis of Ground Contribution to Fallout Penetration of Simple Structures

UNCLASSIFIED

Security Classification

DOCUMENT CONTROL DATA - R&D

(Security classification of title, body of abstract and indexing annotation must be entered when the overall report is classified)

1 ORIGINATING ACTIVITY (Corporate author)

University of Illinois
Urbana, Illinois

2a REPORT SECURITY CLASSIFICATION

Unclassified

2b GROUP

3 REPORT TITLE

A COMPARISON OF THEORY AND EXPERIMENT FOR SHIELDING BY A STRUCTURE AGAINST FALLOUT RADIATION

4 DESCRIPTIVE NOTES (Type of report and inclusive dates)

Final June 1965 - June 1966

5 AUTHOR(S) (Last name, first name, initial)

Preiss, Kenneth
Chilton, Arthur B.

6 REPORT DATE	7a TOTAL NO OF PAGES	7b NO OF REFS
June 1966	52	17

8a CONTRACT OR GRANT NO	9a ORIGINATOR'S REPORT NUMBER(S)
OCD OS 63 66	Nuclear Radiation Shielding Studies Report No. 1
b PROJECT NO	
c	9b OTHER REPORT NO(S) (Any other numbers that may be assigned this report)
d	NRSS 1

10 AVAILABILITY/LIMITATION NOTICES

Distribution of this document is unlimited.

11 SUPPLEMENTARY NOTES	12 SPONSORING MILITARY ACTIVITY
	Office of Civil Defense Department of the Army Washington, D. C.

13 ABSTRACT

Shielding, fallout, radiation exposure.

Experimental results for exposure penetrating a roof ab, and for reduction factor, are found to agree with moments theory calculations, often to better than 10% when the geometry factor $L_a(\omega,X)$ is used.

Errors in comparing experiment and theory, due to anisotropy of the experimental source, to lack of source reflection in roof experiments, and due to error in estimating the thickness of the roof, are found to be small, but not necessarily negligible.

Detailed results of penetration in iron and concrete, due to plane isotropic sources of various energies are given and a review of ground contribution to fallout radiation penetration through simple structures is appended.

DD FORM 1 JAN 64 1473

Unclassified

Security Classification